Reprinted from JOURNAL OF PHYSICAL OCEANOGRAPHY, Vol. 25, No. 6, Part I, June 1995
American Meteorological Society

Assimilation of Altimeter Data into a Quasigeostrophic Model of the Gulf Stream System. Part II: Assimilation Results

ANTONIETTA CAPOTONDI*

MIT-WHOI Joint Program, Cambridge, Massachusetts

WILLIAM R. HOLLAND

National Center for Atmospheric Research,† Boulder, Colorado

PAOLA MALANOTTE-RIZZOLI

Massachusetts Institute of Technology, Cambridge, Massachusetts

(Manuscript received 21 June 1993, in final form 14 September 1994)

ABSTRACT

The improvement in the climatological behavior of a numerical model as a consequence of the assimilation of surface data is investigated. The model used for this study is a quasigeostrophic (QG) model of the Gulf Stream region. The data that have been assimilated are maps of sea surface height that have been obtained as the superposition of sea surface height variability deduced from the Geosat altimeter measurements and a mean field constructed from historical hydrographic data. The method used for assimilating the data is the nudging technique. Nudging has been implemented in such a way as to achieve a high degree of convergence of the surface model fields toward the observations.

Comparisons of the assimilation results with available in situ observations show a significant improvement in the degree of realism of the climatological model behavior, with respect to the model in which no data are assimilated. The remaining discrepancies in the model mean circulation seem to be mainly associated with deficiencies in the mean component of the surface data that are assimilated. On the other hand, the possibility of building into the model more realistic eddy characteristics through the assimilation of the surface eddy field proves very successful in driving components of the mean model circulation that are in relatively good agreement with the available observations. Comparisons with current meter time series during a time period partially overlapping the Geosat mission show that the model is able to "correctly" extrapolate the instantaneous surface eddy signals to depths of approximately 1500 m. The correlation coefficient between current meter and model time series varies from values close to 0.7 in the top 1500 m to values as low as 0.1–0.2 in the deep ocean.

1. Introduction

The major emphasis of data assimilation in oceanography is the achievement, through the blending of data and models, of a more accurate description of the ocean circulation. In this regard, oceanographic data assimilation studies differ from the ones performed in the meteorological context, which are mainly focused on prediction issues (Ghil and Malanotte-Rizzoli 1991). Only recently there have been some attempts to use data assimilation techniques for nowcasting and forecasting purposes (Mellor and Ezer 1991; Ezer et al. 1992, 1993). The reason for this difference is in part associated with the limited data basis available to oceanographers with respect to the much larger observational network that has traditionally characterized the meteorological scenario. Therefore, numerical models of the ocean circulation have been considered as fundamental tools for reconstructing observed flow features and for illustrating the associated physical processes. In particular, the accuracy of the model climatological behavior is becoming an increasingly crucial issue in the context of climate studies, where a "realistic" behavior of the oceanic component is an indispensable ingredient for achieving a meaningful coupling with the atmospheric part of the climate model. However, the degree of realism of ocean model climatologies is a very challenging issue. Several studies devoted to model–data intercomparison (Holland and Schmitz 1985; Schmitz and Holland 1986; Thompson and Schmitz 1989; Ezer and Mellor 1992) have shown,

* *Current affiliation:* National Center for Atmospheric Research, Boulder, Colorado.

† The National Center for Atmospheric Research is sponsored by the National Science Foundation.

Corresponding author address: Dr. Antonietta Capotondi, Advanced Study Program, National Center for Atmospheric Research, P.O. Box 3000, Boulder, CO 80307-3000.

in fact, how critical the dependence of the model behavior is on geometry, frictional parameterizations, and boundary conditions, as well as thermodynamic forcing. In particular, in eddy-resolving models these factors seem to affect, in a complex and still not fully understood fashion, the internal processes of eddy–mean flow interaction. As a consequence, model-derived climatologies of the mean circulation and of the eddy field often disagree with the perception of the ocean climatology that is derived from the available observations.

In this study we investigate the possibility of improving the climatological behavior of a multilayer model by constraining the model with surface data. The model is a quasigeostrophic model of the Gulf Stream region. The surface data consist of measurements of sea surface height collected in the context of the Geosat mission. Both model and data have been described in detail in Capotondi et al. (1995, hereafter Part I). In Part I we have developed a dynamical framework for rationalizing the consequences of applying to the model a surface streamfunction boundary condition, which is equivalent to a surface pressure boundary condition. In Part II we try to verify the success of this data assimilation procedure implementation. The specific question that we address in this paper is the following: how "realistic" are the subsurface fields that the model develops? That is, how effective are surface data in improving the model behavior? To answer this question we present the comparison between the results of the assimilation experiment and some of the available observations. In this regard we consider the experiment in which the total (mean plus eddies) surface streamfunction is assimilated. This experiment has been described in Part I.

As emphasized in Part I, the approach we have adopted in this study is to assume complete and uniformly accurate surface information. Although appropriate for understanding the dynamical implications of a surface pressure boundary condition as discussed in Part I, this assumption needs some further comments in the present context. In fact, the surface data that we assimilate cannot be expected to be uniformly accurate. They include a mean component that has been derived from climatological hydrographic data by using the dynamic method. The choice of such a long-term mean field as the missing mean component of the Geosat data set, which is only two years long, represents a likely source of error, as well as the assumptions involved in the application of the dynamic method. The altimeter data, on the other hand, have a space–time resolution that cannot be expected to resolve all the dynamically relevant scales (Wunsch 1989b). Space–time interpolation of these data allows the definition of eddy streamfunction values at each model grid point and at time intervals short enough to justify a continuous assimilation in time. However, the accuracy of these objectively created maps is not uniform, but it varies in space as a function of the original data distribution (Wunsch 1989a). Therefore, when considering the comparison with other independent observations, we need to consider the limitations of the surface streamfunction fields ψ_{obs} that have been assimilated. In the spirit of this study, we omit a rigorous error analysis. Our approach here is to consider the maps of ψ_{obs} as a better description of the surface ocean circulation with respect to the one derived from the unconstrained model. However, to be able to assess the impact of inaccuracies in ψ_{obs} on the assimilation results, we discuss in section 2 the capability of the interpolated Geosat data to capture basic aspects of the surface eddy fields.

To better appreciate the comparison with observations, we briefly describe in section 3 the characteristics of the model climatology when no surface data constraint is applied. This numerical simulation, which represents a control model run, is started from the same initial conditions used in the assimilation experiments and uses the same boundary conditions, as well as the same forcing and friction coefficients. It is, therefore, completely equivalent to the assimilation experiments except for the absence of any surface data constraint.

The comparison with observations is presented in section 4. We consider aspects of the mean circulation, as well as aspects of the eddy climatology, including position and intensity of the mean Gulf Stream and its southern recirculation and distribution of eddy kinetic energy with depth. A large part of our analysis is devoted to the comparison of the results of the assimilation experiment with the current meter data from the SYNOP east array. These data were collected during a period of time partially overlapping the Geosat mission. They are available at different locations within the Gulf Stream system and at different depths, the shallowest being about 250 m and the deepest about 4000 m. This dataset, thus, offers a unique opportunity for investigating how the surface eddy signal is "projected" downward at different depths and how "realistic" the deep signature of the surface eddy information is.

We conclude in section 5 with a dynamical interpretation of these comparisons and a discussion of the results.

2. The assimilated eddy fields

The Geosat dataset, as well as the interpolation procedure used for creating eddy streamfunction maps at constant time intervals, has been described in Part I. Here we discuss the capability of these maps to capture basic features of the surface eddy field. As an example of a typical interpolated map, we show in Fig. 1a the eddy streamfunction field corresponding to 6 January 1987. The spatial distribution of the data used for creating that map is shown in Fig. 1b. This distribution corresponds to the data available in the area in a time

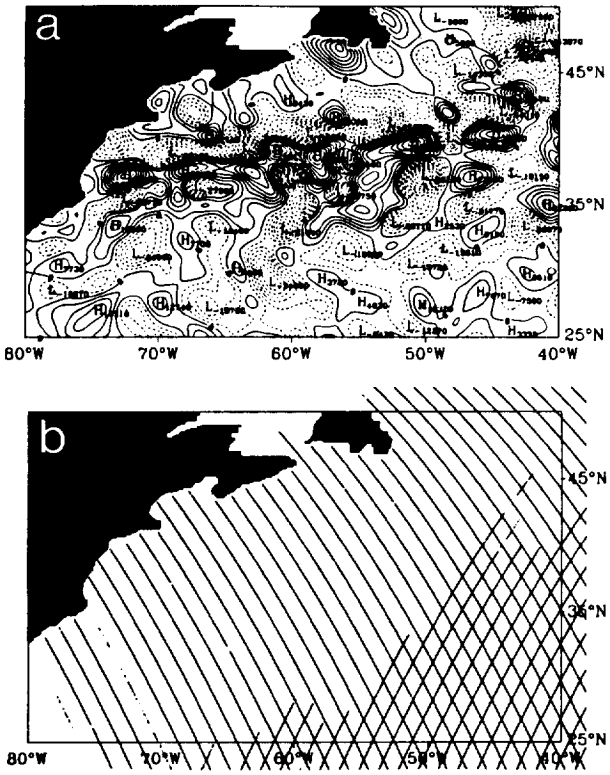

FIG. 1. (a) Example of eddy streamfunction field obtained by space–time interpolation of the Geosat data. It corresponds to the day 6 January 1987. (b) Spatial distribution of the Geosat data used for creating the eddy field in (a). The data are relative to a time period of 34 days centered at 6 January 1987.

window of 34 days centered on the day of the analysis. Most of the data are concentrated along the ascending tracks. In fact, most of the descending tracks are missing in this area due to a malfunctioning of the altimeter. Note that the distribution of the eddy field in Fig. 1a is suggestive of the mean position of the Gulf Stream.

One of the reasons for choosing the Gulf Stream as the study area was associated with the availability in this region of in situ observations collected during a period of time partially overlapping the Geosat mission as part of the SYNOP (Synoptic Ocean Prediction) experiment. These observations allow the verification of the Geosat data, as well as the verification of the assimilation results at different depths. For this purpose we consider the current meter measurements at the SYNOP east array (N. Hogg, 1991, personal communications) centered around 55°W. The SYNOP East Array was deployed from September 1987 to August 1989. Each of the moorings included a minimum of two current meters located around 500 and 4000 m. Some of the moorings were equipped with current meters at additional depths of about 250 m, 1000 m, and 1500 m. The location of the moorings and the depths of the relative current meters (as supplied by N. Hogg) are given in Table 1. The position of the moorings in the Gulf Stream region (also supplied by N. Hogg) is shown in Fig. 2. The data consist of daily averages of zonal and meridional velocity components. The temporal mean has been removed for comparison with the time-dependent part of the altimetric fields. Similar time series for the zonal and meridional surface geostrophic velocities were computed from the bidaily eddy streamfunction fields obtained from the statistical interpolation of Geosat data, starting from September 1987.

In Figs. 3 and 4 we show as typical examples the comparison of the time series at two different locations at the same longitude of 54.67°W. The first location (Fig. 3) is the one at 40.87°N; the second (Fig. 4) is

TABLE 1. Mooring information for the SYNOP East Array (courtesy of N. Hogg). The first column is the experiment mooring number. The second column is the Buoy Group's consecutive mooring number. The depths were computed by using program NOYFB.

Mooring EXP/BUOY		Lat (deg min N)	Long (deg min W)	Water depth (m)	Duration from 9/87 (day)	Duration to 8/89 (day)	Current meter nominal depths (m)				
1	857	41 36.2	54 39.0	4877	20	24	269	522			4018
2	858	40 51.4	53 41.6	5090	21	23	244	497			3992
3	859	40 51.7	54 40.0	5062	21	24	247	500	1008	1516	3995
4	860	40 52.4	55 40.2	5091	22	25		485			3996
5	861	40 08.0	54 40.2	5193	23	23		499	1007	1510	3997
6	862	39 23.0	53 38.9	5252	24	22		485			3997
7	863	39 24.0	54 34.8	5258	25	21		499	1006	1510	3996
8	864	39 23.8	55 40.4	5259	27	20		484			3995
9	865	38 34.9	54 40.3	5331	27	19		500	1007	1511	3997
10	866	37 52.3	53 40.0	5386	28	17	246	500			3995
11	867	37 48.1	54 39.9	5375	29	16	252	505	1012	1520	3999
12	868	37 00.2	54 40.2	5404	29	15	247	500			3996
13	869	37 48.0	55 39.9	5339	30	13		497			4008

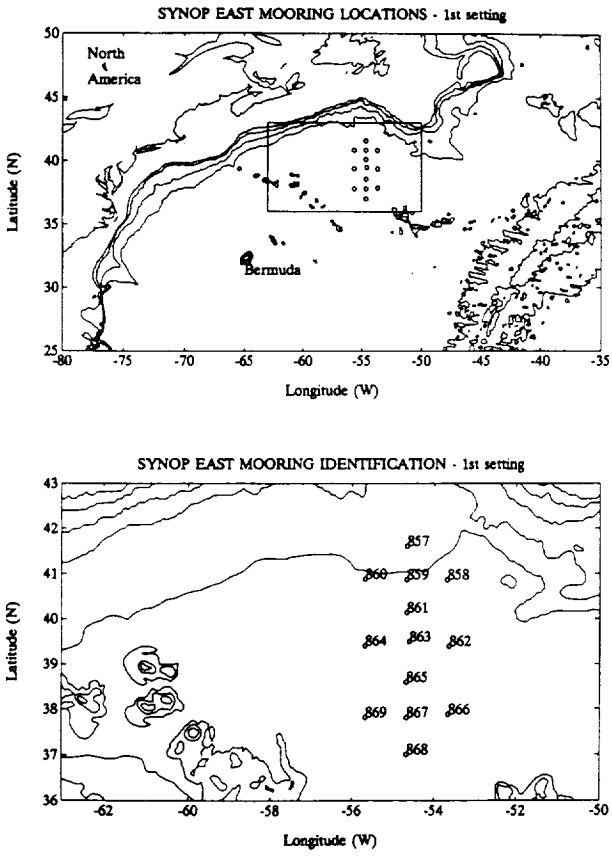

FIG. 2. Position of the moorings (bottom panel) at the SYNOP East Array within the Gulf Stream area (top panel). (Courtesy of N. Hogg.)

at 37°N. The depth of the current meters used for the comparison is 247 m at both moorings. Figures 3a and 4a represent the zonal velocity, and Figs. 3b and 4b the meridional velocity. In all figures the solid line represents the current meter time series, while the dotted line represents the evolution of the geostrophic velocities. Day 0 in the abscissa corresponds to 1 September 1987.

In both examples the comparison shows striking similarities in the general behavior of the two time series. In particular, the most energetic, low-frequency events present in the current meter records can be observed also in the geostrophic velocities. This result is even more remarkable considering that at least 50% of the Geosat data is missing in this area with respect to the expected data coverage for a perfect altimeter operation. Also, we are comparing surface geostrophic velocities with total velocities measured at some depth below the surface. In the time series at 37°N, peak velocities obtained with the Geosat data are often less than the ones observed in the current meter data. At both locations we can often observe a phase shift. Also, the surface velocity time series are generally smoother than the current meter time series. These characteristics can be considered a consequence of the space–time interpolation of the altimeter data. These qualitative considerations are supported by a spectrum analysis of the time series (Capotondi 1993). In fact, the spectra obtained from the geostrophic velocities are quite similar, both in shape and energy level, to the ones obtained from the current meter measurements at the depth of approximately 250 m. However, the geostrophic velocity spectra tend to decrease faster, at periods shorter than approximately 30 days, than the corresponding current meter spectra. Although consistent with the temporal smoothing associated with the interpolation procedure, the higher energy in the current meter measurements could be partially attributed to the presence of ageostrophic motion associated with high-frequency meandering processes (Johns et al. 1989), as well as with the lack of information content of the surface geostrophic velocity time series at periods shorter than the Geosat Nyquist period (34 days). The coherence between the geostrophic velocity time series and the current meter time series is found to be much above the significance level (Capotondi 1993) for periods longer than approximately 30 days. In this frequency range phase shifts are very small.

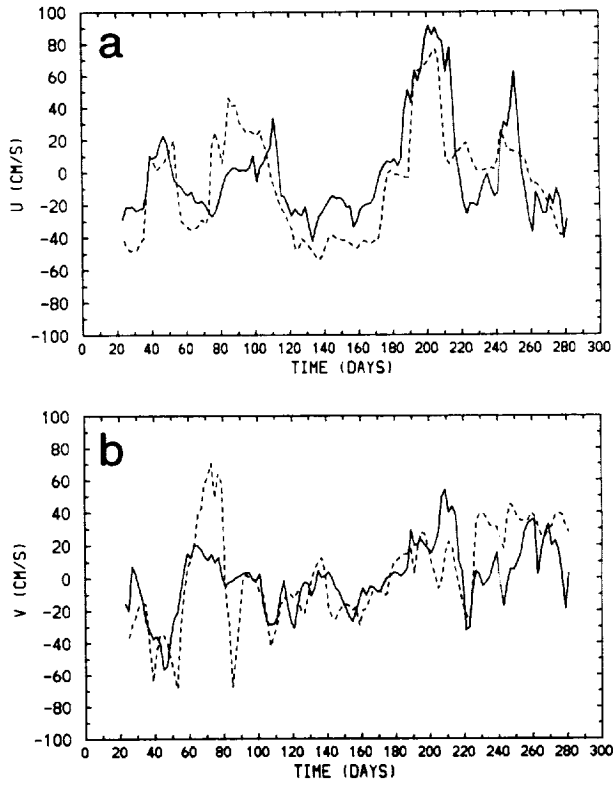

FIG. 3. Comparison of velocity time series at 40.87°N, 54.67°W. The solid line represents current meter measurements at 247-m depth. The dashed line represents the time evolution of the geostrophic velocity derived from the interpolated Geosat maps, available at 2-day intervals. (a) Zonal velocity components. (b) Meridional velocity components.

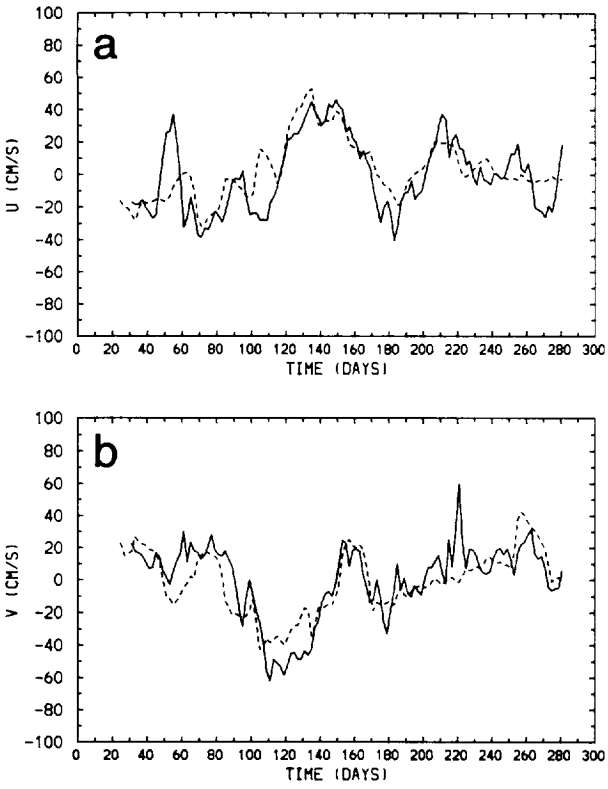

FIG. 4. Same as in Fig. 3 but at 37°N, 54.67°W.

The eddy kinetic energy level and distribution is one of the quantities that models are often not able to reproduce correctly (Schmitz and Holland 1982; Schmitz and Thompson 1992). One of the aspects we want to analyze in this work is the way the model extrapolates the eddy intensity of the surface data to the subsurface layers. Therefore, we are interested in assimilating surface data with the "correct" energy level. The eddy kinetic energy distribution calculated geostrophically from our statistically interpolated fields is shown in Fig. 5a. It has been compared both with the "classical" map of surface eddy kinetic energy constructed by Richardson from surface drifter data (Richardson 1983b) and with the eddy kinetic energy distribution computed by Le Traon et al. (1990) from Geosat data themselves. Richardson's estimate of surface eddy kinetic energy (Richardson 1983b), obtained from data averaged over 2° × 2° squares, is reproduced in Fig. 5b.

The general pattern of eddy kinetic energy distribution is very similar in all three cases: the area of highest values is centered around the position of the mean Gulf Stream and follows the stream path around the Grand Banks. The eddy energy decreases away from the stream to values of about 200 $cm^2 s^{-2}$, which are found in the gyre interior, south of the stream, and along the continental shelf area to the north. The maximum of about 1000 $cm^2 s^{-2}$ found by Richardson (1983b) in the Newfoundland basin is also present in our results.

The main discrepancy between Fig. 5a and the corresponding maps prepared by the other authors is in the reduced peak values in the area between 60° and 70°W. In fact, in this area Richardson (1983b) finds values greater than 2000 $cm^2 s^{-2}$ with isolated maxima higher than 3000 $cm^2 s^{-2}$. In the results of Le Traon et al. (1990), the area with values greater than 2000 $cm^2 s^{-2}$ is even larger than in Richardson's (1983b). The values we find, on the other hand, are slightly smaller than 2000 $cm^2 s^{-2}$ with an isolated maximum of about 2400 $cm^2 s^{-2}$ at 38°N, 64°W. The reason for our smaller values is clearly in the smoothing effect produced by the statistical interpolation, which filters out small scales, especially the spatial ones contained by the data in the alongtrack direction. This is illustrated in Fig. 6, where two of the original profiles of sea surface height (solid line) along the tracks shown in Fig. 6c are compared with the ones obtained by reprojecting the interpolated data on the same days along the same tracks. The abscissa in the figures gives the increasing latitude along the ascending tracks. We can see that the finer scales have been removed and the peak values reduced.

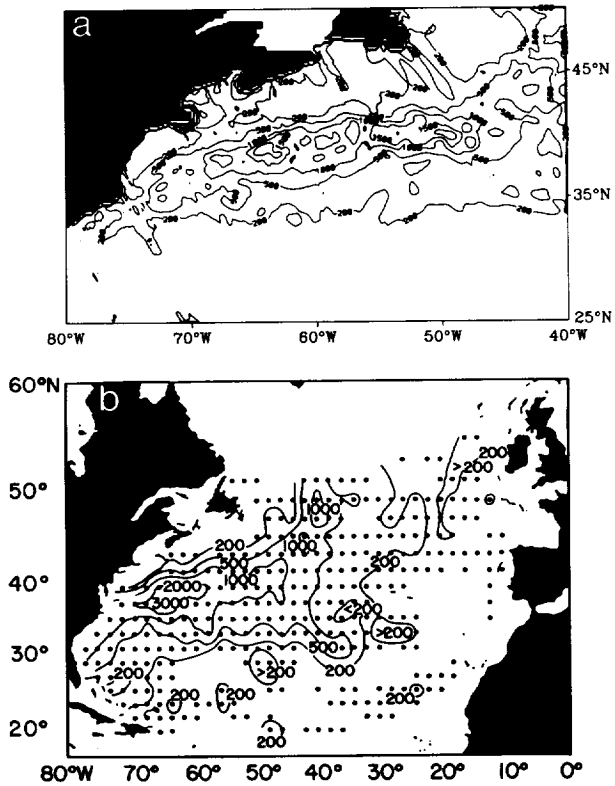

FIG. 5. (a) Eddy kinetic energy distribution derived from the interpolated Geosat data. (b) Surface eddy kinetic energy distribution computed by Richardson from drifter data based on values in 2° × 2° boxes. The dots show location of boxes containing more than 20 observations. Reproduced from Richardson (1985).

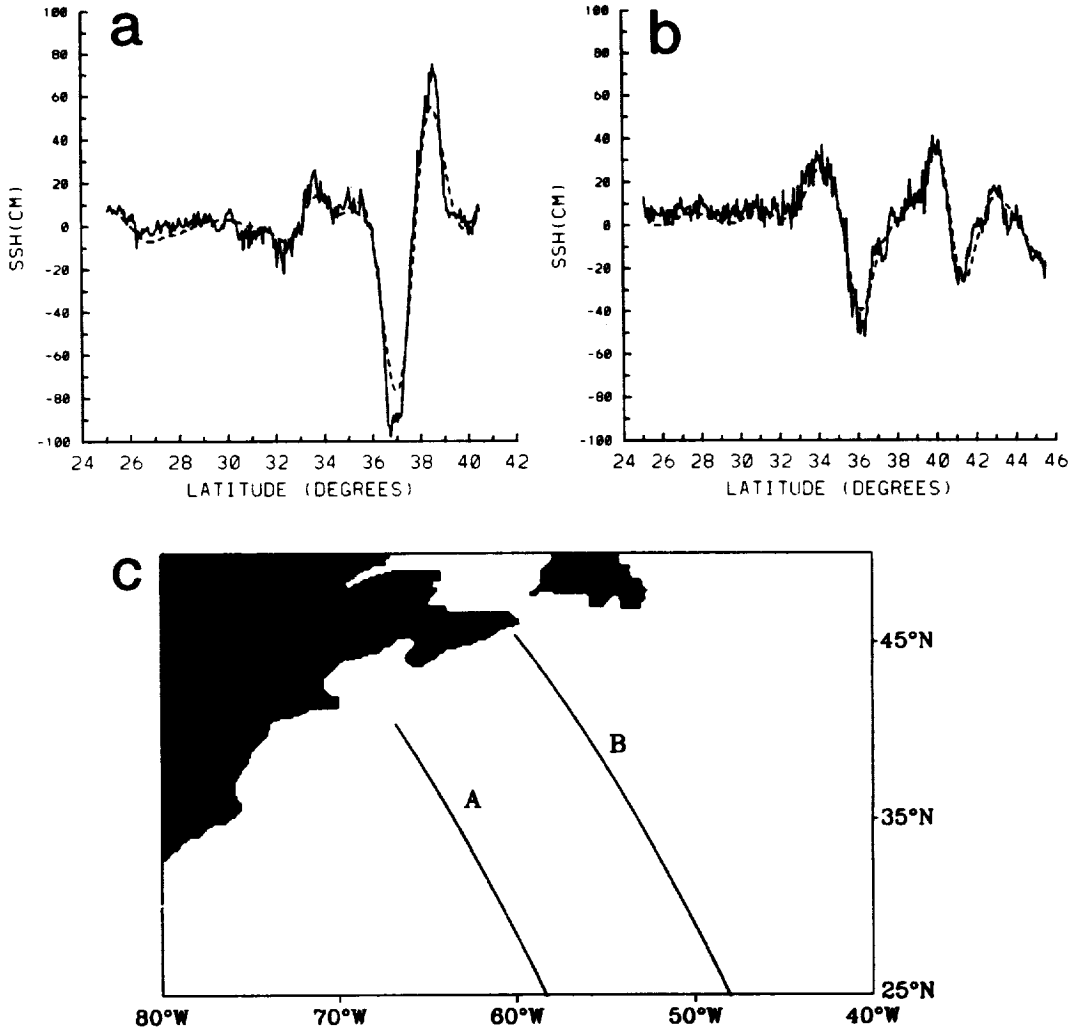

FIG. 6. Comparison between alongtrack sea surface height profiles before (solid line) and after (dashed line) the interpolation. (a) Profiles along the track indicated with "A" in panel (c). (b) Profiles along the track indicated with "B" in panel (c). (c) Representation of the Geosat ground tracks considered for this comparison.

The consequences of the interpolation procedure on the characteristics of the wavenumber spectra are illustrated in Fig. 7, where we compare the wavenumber spectra in the alongtrack direction obtained from the original data (solid lines) with the corresponding spectra obtained from the interpolated data (dotted lines). Eighteen repeats, at intervals of 34 days, have been used for the evaluation of the spectra in Fig. 7. The two panels correspond to the same two tracks shown in Fig. 6c with panel a(b) corresponding to track A(B). The spectra from the interpolated data are practically coincident with the spectra from the original data at wavelengths longer than approximately 240 km, while at shorter wavelengths the energy level is considerably reduced. These results are also consistent with the analysis of Ezer et al. (1993) on the effects of the interpolation parameters on the amplitude of the variability.

The procedure adopted by Le Traon et al. (1990) was to compute the geostrophic velocities and the associated kinetic energy directly from the alongtrack slopes assuming isotropy. They then averaged the kinetic energy values in 2° squares and performed an optimal interpolation to map them. The reduced gradients in the sea surface height profiles in the alongtrack direction resulting from the statistical interpolation procedure, therefore, can explain the differences between our results and the results of Le Traon et al. (1990). We should notice, however, that the maximum values of eddy kinetic energy seem to be very sensitive to the particular procedure used to average the data in space and time. In fact, the map of eddy kinetic energy obtained by processing the drifter data in the same way as the Geosat data (Le Traon et al. 1990) shows reduced peak values, which are very similar to the ones we obtain. We can conclude, therefore, that the eddy kinetic

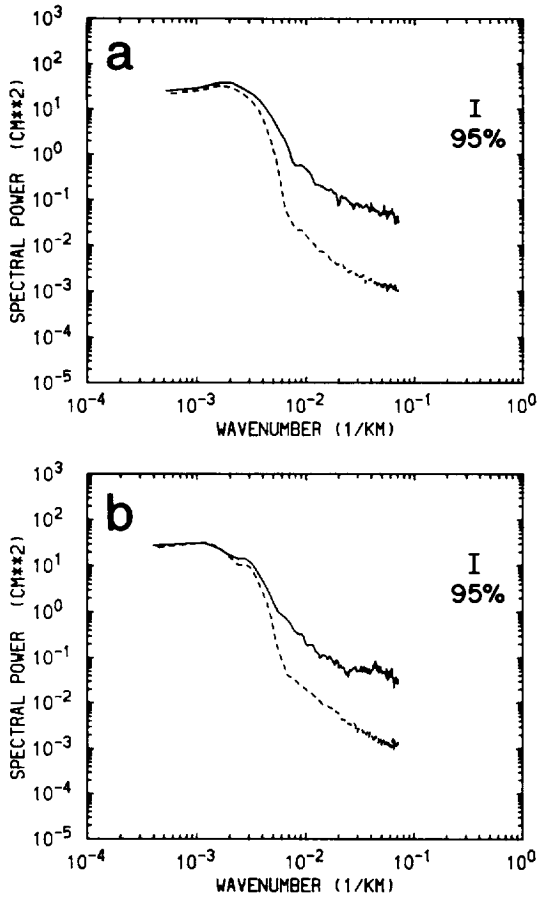

FIG. 7. Comparison between alongtrack wavenumber spectra before (solid line) and after (dashed line) the interpolation. (a) Average wavenumber spectra computed from 18 sea surface height profiles, at 34-day intervals, along the Geosat track indicated with "A" in Fig. 6c. (b) Average wavenumber spectra computed from 18 sea surface height profiles, at 34-day intervals, along the Geosat track indicated with "B" in Fig. 6c. The 18 profiles of SSH are considered statistically independent. We have also performed a running average over three wavenumber bins in the periodograms. This leads to approximately 90 degrees of freedom, which is the value used to compute the confidence interval shown in the figures.

energy distribution associated with the interpolated data that we are going to assimilate into the model can be considered in reasonably good agreement with the other available estimates of this quantity.

3. The "control run"

This numerical experiment is started from the same initial conditions used for the assimilation experiments as described in Part I: layers 1, 2, and 3 are initialized with the climatological fields shown in Fig. 1 of Part I, while the two bottom layers are motionless. The climatological fields also supply the streamfunction distributions along the open boundaries of layers 1, 2, and 3 that are used as boundary conditions in all experiments. A detailed description of the boundary conditions is given in Part I. The numerical simulation has been carried out for 20 years to allow the model fields to reach a statistical equilibrium. We have monitored the evolution of the total kinetic energy for assessing the achievement of the statistical steady state. The climatology of this model has been computed over the last four years of the numerical integration.

The mean streamfunction fields in the five model layers are shown in Fig. 8. In the three upper layers, we notice the mean Gulf Stream entering at the western boundary as a thin boundary jet, overshooting at Cape Hatteras before leaving the coast, and flowing eastward as an almost zonal jet. Two very intense inertial recirculation gyres are observed in the western half of the domain. They seem to be responsible for the rapid depletion of the jet and for its limited penetration scale. Experiments performed by Marshall and Marshall (1992) with a reduced gravity model suggest that the characteristics of the inertial recirculation and the consequent penetration scale of the jet can be affected by the boundary condition used to describe the jet entering at the western boundary. The rationale behind their results is that the profile chosen for the jet at the western boundary establishes a relationship between streamfunction and potential vorticity with a given value of the parameter $\alpha = dq/d\psi$. Depending on the sign of α, either Fofonoff-like solutions ($\alpha > 0$) or modonlike solutions ($\alpha < 0$) can be excited in a resonant fashion. In the first case the jet can cross the whole domain, while in the second case a tight recirculation close to the western boundary is expected. The characteristics of the recirculation in our solution are consistent with these results, even if the context of the present model simulation is more complex than the simple idealized experiment of Marshall and Marshall. In the interior the recirculation appears broader and suggestive of the Sverdrup balance. An auxiliary experiment performed with the wind stress turned off (Capotondi 1993) confirms, in fact, the wind-driven nature of the interior recirculation. The position of the eastward flowing jet, on the other hand, appears associated with the outflow boundary conditions prescribed at the eastern boundary. The broad nature of this outflow, as well as the absence of any northern recirculation gyre inflow at the eastern boundary, are responsible for the flow tendency to "fill" the northern half of the domain. The branch of the stream that reaches the northern boundary is forced to recirculate in a tight gyre, almost barotropic in character, by the no-flow conditions prescribed at this boundary.

All the above features of the mean circulation (separation of the Gulf Stream from the coast, zonal character of the eastward flowing jet, inertial recirculation much too intense and localized in the western half of the domain, recirculation gyre at the northern boundary) appear in disagreement with the perception of the mean circulation in this area that is derived from observations. It is important to emphasize that no attempt

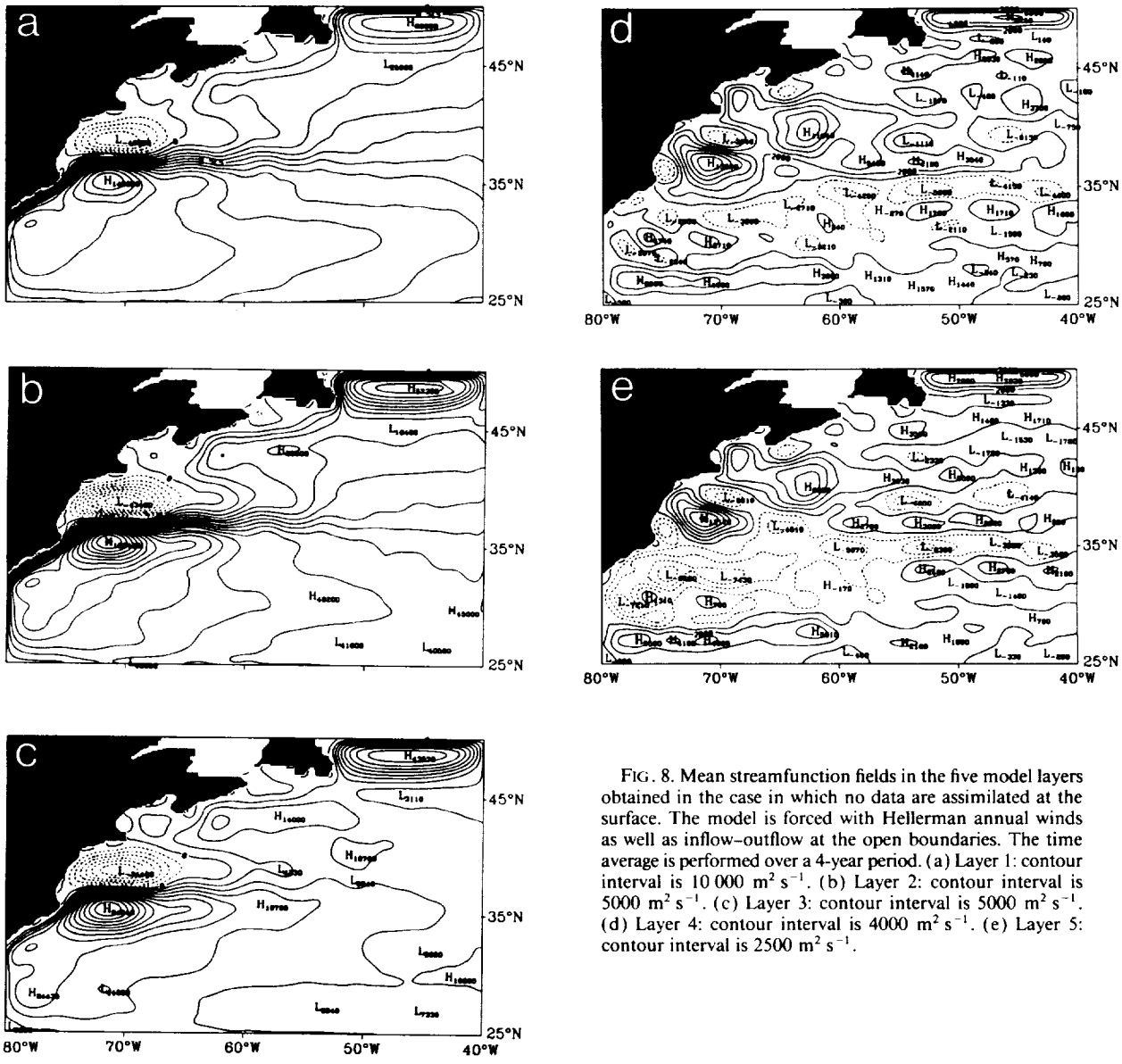

FIG. 8. Mean streamfunction fields in the five model layers obtained in the case in which no data are assimilated at the surface. The model is forced with Hellerman annual winds as well as inflow–outflow at the open boundaries. The time average is performed over a 4-year period. (a) Layer 1: contour interval is 10 000 $m^2 s^{-1}$. (b) Layer 2: contour interval is 5000 $m^2 s^{-1}$. (c) Layer 3: contour interval is 5000 $m^2 s^{-1}$. (d) Layer 4: contour interval is 4000 $m^2 s^{-1}$. (e) Layer 5: contour interval is 2500 $m^2 s^{-1}$.

has been made to improve some aspects of the model climatology by a proper "tuning" of the model parameters, in particular friction and boundary conditions. Improving ocean models is obviously a necessary and continuing effort. However, our major interest here is to analyze the changes introduced by the assimilation of surface data in a given ocean model. Therefore, we have used the exact same boundary conditions and viscosities in all experiments.

Since no data are assimilated in this experiment, the eddy field that characterizes this model simulation is produced by the natural barotropic and baroclinic instabilities that occur in the model. As an example, Fig. 9 shows a typical instantaneous state on a particular day toward the end of the integration. Only the streamfunctions for the first, third, and fifth layer are shown for brevity. The far field is dominated by intense eddies of barotropic nature, whose characteristic length scales appear to be much larger than the ones typical of ocean variability (Le Traon et al. 1990). Wavenumber spectra of the model sea surface height variability along some of the Geosat tracks yield mean wavelengths two to three times larger than the ones derived from wavenumber spectra of the Geosat data themselves (Capotondi 1993).

The most energetic part of the flow, including the strong westward flow associated with the inertial recirculation gyres, seems to be confined in all five layers to the western half of the domain. Therefore, we may expect that the instability processes leading to eddy production will mainly take place in this area. Figure

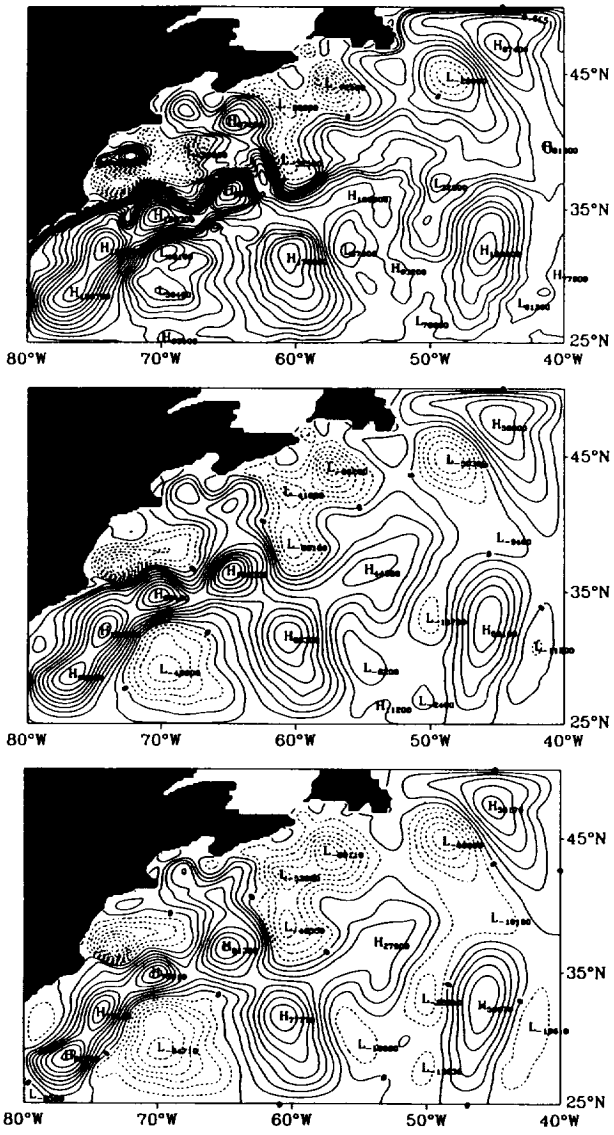

FIG. 9. Instantaneous streamfunction fields on a day toward the end of the 20-year integration. Only layer 1 (top), layer 3 (middle), and layer 5 (bottom) are shown.

10 shows, in fact, the eddy kinetic energy distribution within the model domain. A large pool of high eddy kinetic energy, up to values of 6000 $cm^2 s^{-2}$ in layer 1, is found in the western part of the domain. A tongue of maximum values extends a bit north of Cape Hatteras and then mainly eastward centered upon 37°N. The tongue of high values is oriented along the stream path. This is especially evident in layer 1. The eddy kinetic energy levels in all layers maintain relatively high values in much of the domain due to the presence of large barotropic eddies. By comparison with the "classical" picture of surface eddy kinetic energy distribution prepared by Richardson (1983b) and reproduced in Fig. 5b, it is immediately evident that the corresponding map obtained from the model simulation (Fig. 10a) is far from realistic both in pattern and intensity. The discrepancy in pattern is obviously associated with the mean position of the model jet, which as mentioned before leaves the coast a little past Cape Hatteras and remains at a latitude that is too far south with respect to the position of the real Gulf Stream. The eddy kinetic energy in the model simulation is at least 50% higher than in Richardson's map. Also at depth the level is far too high when compared with the abyssal eddy kinetic energy picture constructed by Schmitz (1984). These unrealistically high eddy kinetic energy values can be probably explained with intense instability processes taking place in the western half of the domain. In this area, in fact, the model jet is very narrow and energetic, thus favoring barotropic insta-

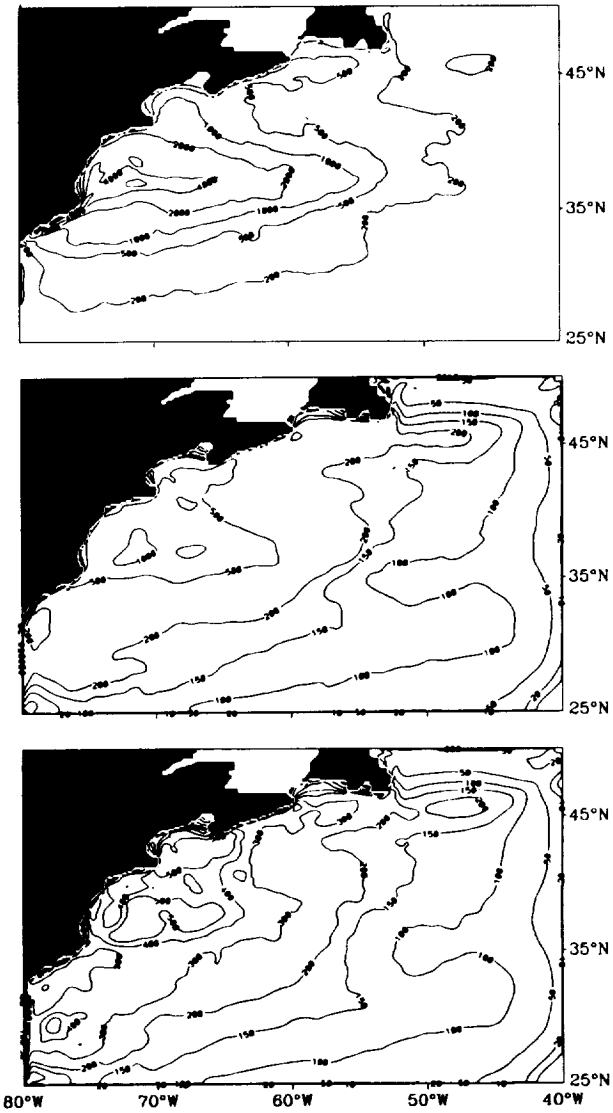

FIG. 10. Eddy kinetic energy distributions in layer 1 (top), layer 3 (middle), and layer 5 (bottom).

bility processes. We also have, in the same area, intense westward flows associated with the inertial recirculation gyres where baroclinic instability is very likely to occur (Pedlosky 1979). The basin-like character of the eddy kinetic energy distribution, especially at depth, can be attributed to the presence of the barotropic eddies mentioned before. In fact, the barotropic disturbances present in the model eddy field tend to organize themselves in the form of basin modes, as shown by a spectral analysis in the frequency domain of the model streamfunction fields (Capotondi 1993). These results suggest a reevaluation of our boundary conditions that should allow radiation of these oscillations in all layers. Spectral analysis also shows the existence of different dynamical regimes as expressed by the geographical variation of the frequency spectra, in analogy with what was found in previous studies of QG models (Lozier and Riser 1990).

The results of this numerical simulation are consistent with previous studies of QG dynamics in idealized domains (Holland 1978; Marshall 1984; Rhines and Schopp 1991) and can be partially understood within that dynamical framework. However, when considering the available observations in this area, several deficiencies in the model behavior emerge. These deficiencies, which in different ways and to different extents are common to any ocean model, are mainly associated with the path of the model stream and with the distribution and intensity of the eddy kinetic energy. From a spectral point of view, the model reveals a high degree of complexity and richness in its spatial and temporal scales. However, the typical model length scales are larger than the ones associated with the mesoscale eddy field in the ocean. Also, a large component of the time-dependent motion is given by barotropic signals that appear to organize themselves in basin-mode structures for which no evidence has been found in observations. In the following section we analyze how this scenario is altered by the assimilation of surface data.

4. Comparison of the assimilation results with observations

The assimilation experiment we consider in this section is the one in which the total surface streamfunction (mean plus eddies) is assimilated into the model. This experiment is described in Part I. The mean streamfunction fields in the five model layers for this experiment are shown in Fig. 11. We concentrate here on the comparison of a few aspects of the mean circulation, as well as on some characteristics of the model eddy field.

a. The mean circulation

A comparison of the mean circulation obtained when no data assimilation is applied (Fig. 8) with the mean circulation obtained when a total surface streamfunction field is assimilated (Fig. 11) shows the effectiveness of surface data, when strongly nudged into the model, in modifying the model behavior in all layers. A more direct comparison is presented in Fig. 12, where we show meridional profiles of mean zonal velocity at 55°W in the five model layers. The solid line represents the results from the assimilation experiments, while the dashed line corresponds to the results from the control run. The dotted line in the panels for the three upper layers defines the mean velocity profiles derived from the climatological fields used as initial conditions in both experiments.

The surface data constraint that is applied to the model during the assimilation experiment produces a substantial change in the mean velocity profiles in all five layers. In the upper layer the solid and dotted lines are almost coincident as a consequence of the strong nudging of the model's upper-layer mean streamfunction field toward the climatological streamfunction field. However, in layers 2 and 3, where the climatological fields are only used as initial conditions, the mean circulation that develops during the assimilation experiment shows enhanced maximum eastward velocity between 40 and 42°N with respect to the initial profiles (dotted line). Notice also the development in these layers of the westward return flow at about 36°N associated with the southern recirculation, which is practically absent in the corresponding climatological profiles. As explained in Part I, this component of the circulation is essentially eddy driven and is quite barotropic in character.

How do these results compare with observations? The Gulf Stream area is probably one of the most studied regions in the World Ocean, so that the observational basis is relatively large, including hydrographic data as well as current meter and float data. Two different representations of the mean velocity structure of the Gulf Stream have been developed from the available observations. The first one is the traditional Eulerian mean in which the time average is performed with respect to a fixed coordinate system. The second representation, which can be defined as the "average synoptic stream" (Hall and Bryden 1985; Hogg 1992), describes the average structure of the flow as viewed in a coordinate frame whose origin is at the instantaneous axis of the meandering jet as it moves as a whole. The surface data that we assimilate contain a mean component that is obtained as an Eulerian time average over a long-term dataset. Therefore, the average Eulerian stream seems to be the most appropriate description to be used for comparison with our assimilation results. In the following, we consider comparisons with three different estimates of the average Eulerian stream, estimates that have been derived from different data and with somewhat different criteria. In this way we hope to identify features of the mean circulation that can be considered robust and to assess their range of variation. The first comparison is with

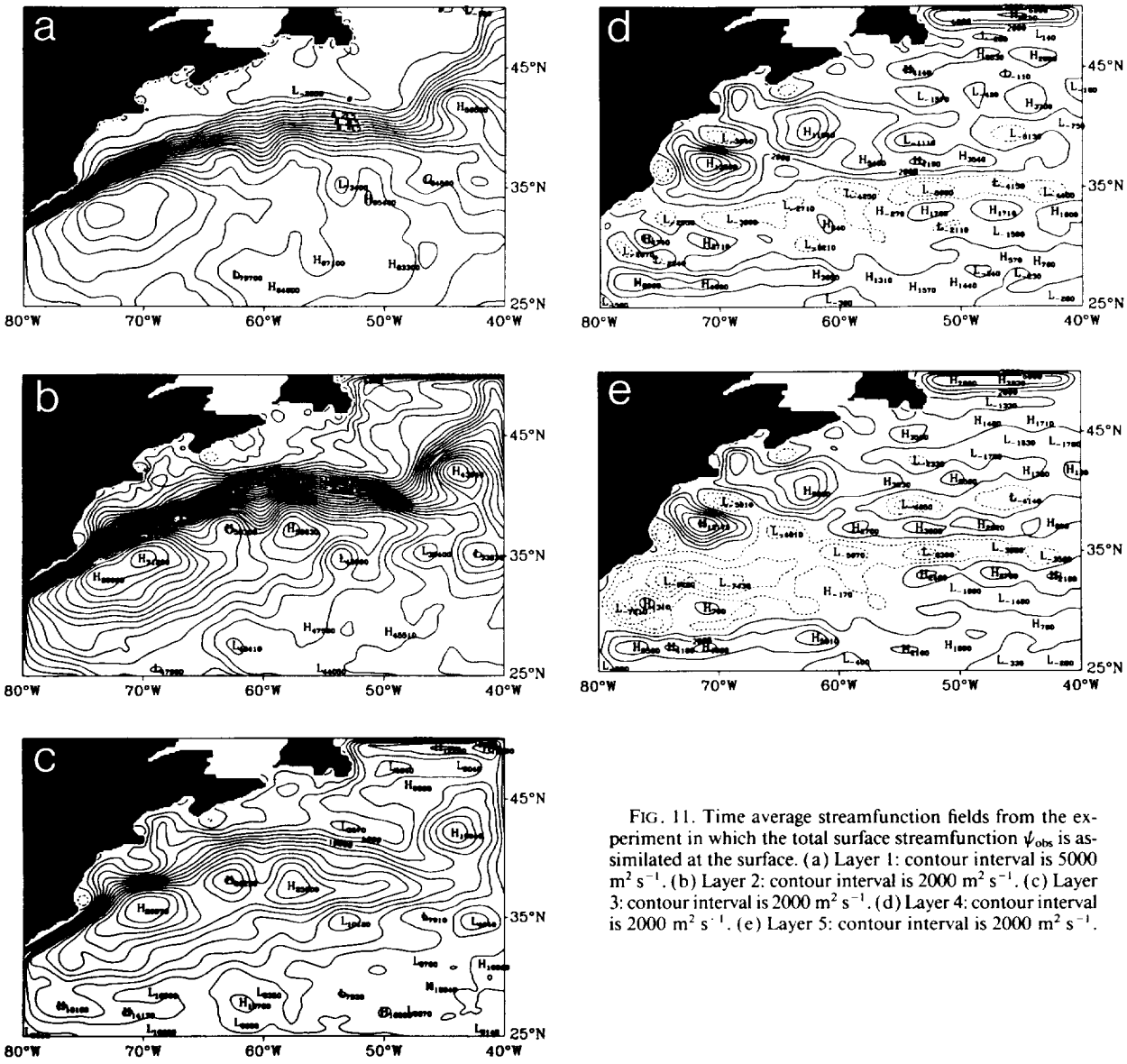

FIG. 11. Time average streamfunction fields from the experiment in which the total surface streamfunction ψ_{obs} is assimilated at the surface. (a) Layer 1: contour interval is 5000 $m^2 s^{-1}$. (b) Layer 2: contour interval is 2000 $m^2 s^{-1}$. (c) Layer 3: contour interval is 2000 $m^2 s^{-1}$. (d) Layer 4: contour interval is 2000 $m^2 s^{-1}$. (e) Layer 5: contour interval is 2000 $m^2 s^{-1}$.

Richardson's section of mean zonal velocity at 55°W (Richardson 1985). The datasets used for this construction include surface drifter data collected in the years 1977–1980, float data at the nominal depths of 700 and 2000 m covering the period 1980–1982, and current meter data at 4000 m from the POLYMODE Array II, which was operating from April 1975 to July 1977. The second comparison is with the mean velocity profiles constructed by Owens (1991) from all the available SOFAR float data at 55°W. These data were collected in the context of several measuring programs. They are available at 700 and 2000 m. Finally, the third comparison is with the mean velocity estimates computed from the current meter measurements at the SYNOP east array. These data have been described in section 2. For this comparison we have considered the time series obtained at the moorings located at approximately 54.7°W (see Table 1 and Fig. 2). Most of the time series are about two years long, the only exceptions being the ones measured near 40°N at 500, 1000, and 1500 m whose duration is only 435 days.

The comparison with Richardson's section is shown in Fig. 13 at the middle depths of the model layers. The estimates computed by Richardson at the surface, 700 m, and 2000 m have been interpolated linearly to the depths of the model layers 1, 2, and 3. The model results for layers 4 and 5 have been compared directly with Richardson's values at 2000 and 4000 m. The estimates from the model have been averaged over 10 degrees of longitude centered at 55°W in analogy with the data processing performed by Richardson. In Fig. 13 the thick solid line describes the velocity profiles

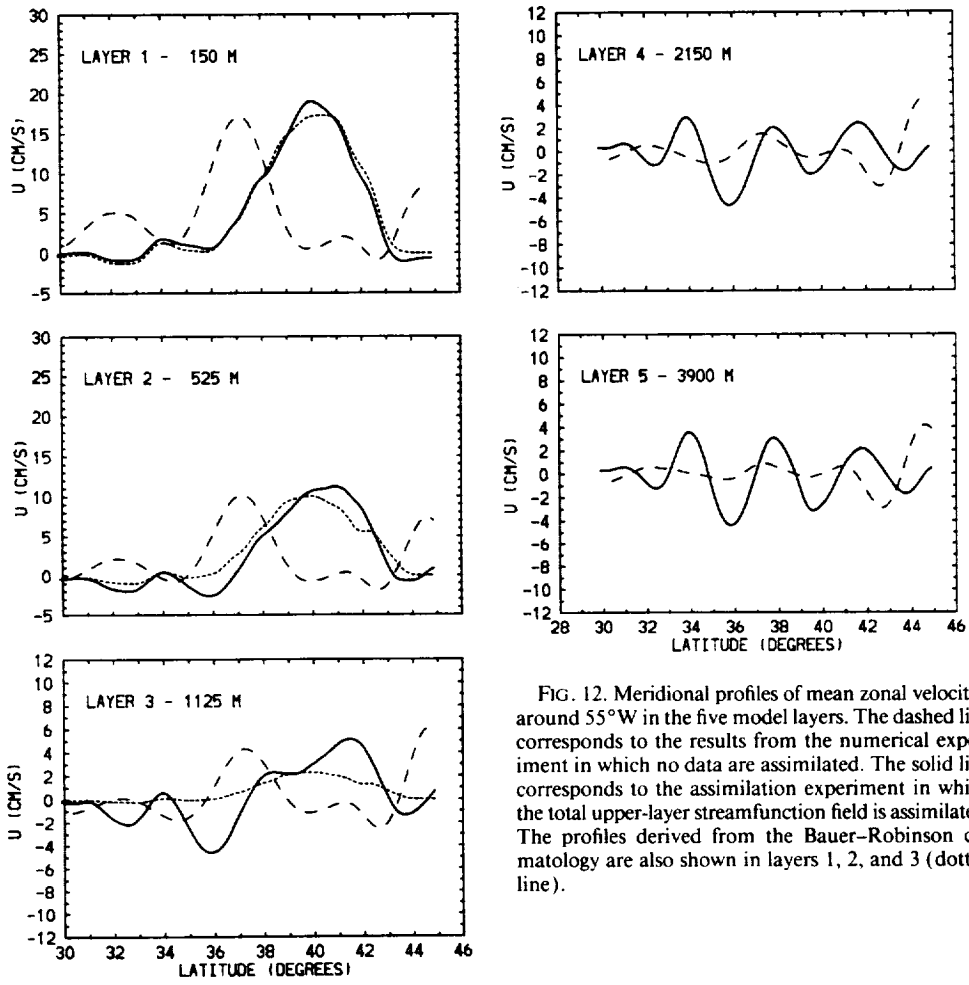

FIG. 12. Meridional profiles of mean zonal velocities around 55°W in the five model layers. The dashed line corresponds to the results from the numerical experiment in which no data are assimilated. The solid line corresponds to the assimilation experiment in which the total upper-layer streamfunction field is assimilated. The profiles derived from the Bauer–Robinson climatology are also shown in layers 1, 2, and 3 (dotted line).

derived from the assimilation experiment, while the dots connected by the thin solid line are derived from Richardson's estimates. The vertical bars indicate the standard error of the mean. In the panels corresponding to layers 1, 2, and 3 the climatological zonal velocity profiles (dotted line) are also shown for reference. In the three upper layers the major discrepancies between assimilation results and Richardson's estimates are found in the width and intensity of the eastward flowing jet. Also, the maximum eastward velocities in these layers appear displaced somewhat northward in the assimilation results with respect to Richardson's profiles. This can be noticed especially in layer 3 where the absolute maximum is found around 41.5°N. These discrepancies can be partially attributed to the characteristics of the surface climatological field that is assimilated as seen in layer 1. In fact, being the result of a long-term average, this field shows an eastward flowing jet broader and weaker than the one obtained by Richardson from surface drifters. A northward displacement of about one degree in the maximum eastward velocity is observed also in the climatological profiles (dotted line). However, the discrepancies observed north of 40°N in layers 2 and 3 appear associated with flow components that develop in the two bottom layers. Notice, in fact, the correlation between the maxima around 38° and 41.5°N in layer 3 with the corresponding maxima in layers 4 and 5.

The position and intensity of the westward flow associated with the southern recirculation are in remarkably good agreement in all five layers. An exception is found in the amplitude of the westward flow in layer 5, where the current meter measurements at 35.5°N show a mean velocity more than twice that obtained in the model. The large amplitude of this westward flow, which appears to be bottom intensified, has been explained by Owens and Hogg (1980) as associated with the Taylor column that develops over a topographic bump. The absence of any topographic relief in the model does not allow bottom intensification in the westward flow at this latitude. We should also notice that the velocity amplitude showed varia-

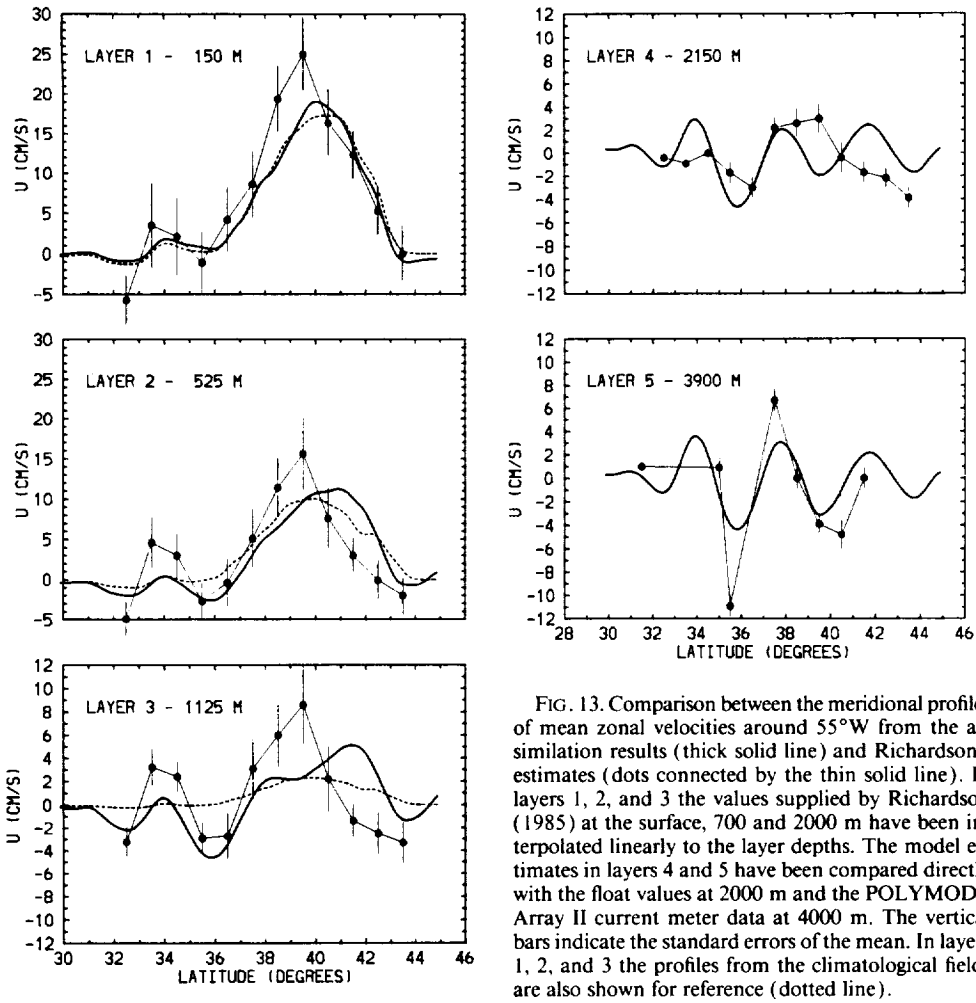

FIG. 13. Comparison between the meridional profiles of mean zonal velocities around 55°W from the assimilation results (thick solid line) and Richardson's estimates (dots connected by the thin solid line). In layers 1, 2, and 3 the values supplied by Richardson (1985) at the surface, 700 and 2000 m have been interpolated linearly to the layer depths. The model estimates in layers 4 and 5 have been compared directly with the float values at 2000 m and the POLYMODE Array II current meter data at 4000 m. The vertical bars indicate the standard errors of the mean. In layers 1, 2, and 3 the profiles from the climatological fields are also shown for reference (dotted line).

tions almost as large as 50% during the three 9-month deployments of the POLYMODE Array II (Schmitz and McCartney 1982). Therefore, the difference we find in the westward flow around 36°N seems to be within the range of the observed variability.

At 4000 m the sequence of zonal jets observed in the model profile is in remarkable agreement with the profile from the POLYMODE current meter measurements over the range of latitude covered by the current meter array. Notice, in particular, the presence in the solid profile of a westward flow around 39°N that represents the model expression of the northern recirculation. Even though no northern recirculation gyre is present in the surface climatological field that is assimilated, the deep flow, which is essentially eddy driven, does have this feature. However, the amplitudes of both the Gulf Stream and its countercurrents are underestimated in the model with respect to the current meter measurements.

In layer 4 the amplitude of the zonal currents is in better agreement with the observations. However, the sequence of alternating jets shown by the solid profile is not fully observed in the data. Only the southern countercurrent, the Gulf Stream, and the northern countercurrent are present in the observation profile. The sequence of zonal jets in model layer 4 appears very similar to the one in layer 5. The flow in the two deeper model layers seems to have a barotropic character that is not found in Richardson's estimates at 2000 and 4000 m. Whether this is a consequence of the different types of datasets used for his estimates (as well as different data processing and different time periods) or a consequence of a model deficiency cannot be determined from the information presently available. However, from the analysis presented in Part I, we may expect unrealistic flow features to develop at latitudes north of the surface climatological Gulf Stream due to the absence of a northern recirculation gyre in this area. Even if the deep flow appears to be an eddy-driven phenomenon, the structure of this flow, including the position of the northern recirculation, is expected

to be controlled by the structure of the surface mean field.

Similar characteristics emerge from the comparisons of the assimilation results with the two other estimates of the mean Eulerian stream that we are considering. The comparison with Owen's velocity profiles at 55°W is shown in Fig. 14, while the comparison with the velocity sections from the SYNOP data is shown in Fig. 15. In these figures the dashed line indicates the model results interpolated linearly at the data depths, whereas the dots connected by the thin solid line are the observational estimates. The standard errors of the mean in Fig. 14 were computed by Owens, assuming a decorrelation time of 20 days (Owens 1991). Those in Fig. 15 have been evaluated in a similar fashion. In both figures the flow is mainly zonal. The model Gulf Stream appears broader and weaker than the one shown by the profiles derived from the observations in the upper 1500 m. This is particularly evident in the comparison with the SYNOP velocity profiles since no spatial averaging has been applied to the current meter data. The float data, on the other hand, have been averaged in latitude–longitude boxes of sufficient extent to ensure statistical reliability (Owens 1991). The differences in the intensity of the eastward flowing jet seem to decrease with depth. In fact, both at 2000 m in Fig. 14 and at 4000 m in Fig. 15, the model signature of the deep Gulf Stream appears to have a peak velocity in good agreement with the observational estimates. This agreement is consistent with the deep flow in the model being essentially eddy driven, as discussed in Part I. Only the position of the different flow features can be related to the mean component of the assimilated data. The deep eddy-driven flow is communicated to some extent to the layers above, as can be seen in Fig. 13: the zonal velocities are practically barotropic in the two bottom layers and strongly correlated with the peak velocities in layers 2 and 3. This "quasi-baro-

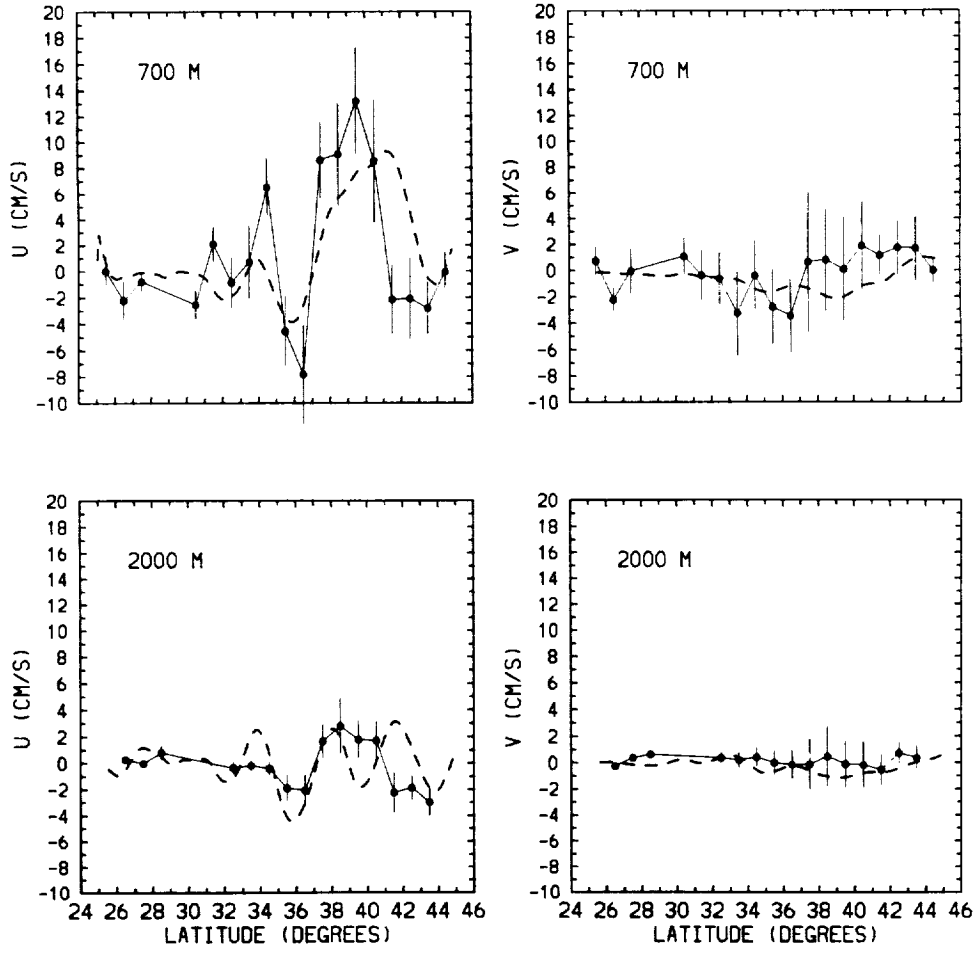

FIG. 14. Comparison between the meridional profiles of velocity components around 55°W from the assimilation results (dashed line) and estimates computed by Owens (1991) from SOFAR float data (dots connected by the thin solid line). The left panels show the zonal velocities at 700 (top) and 2000 m (bottom). The right panels show the meridional velocities at the same depths. Vertical bars indicate the standard error of the mean.

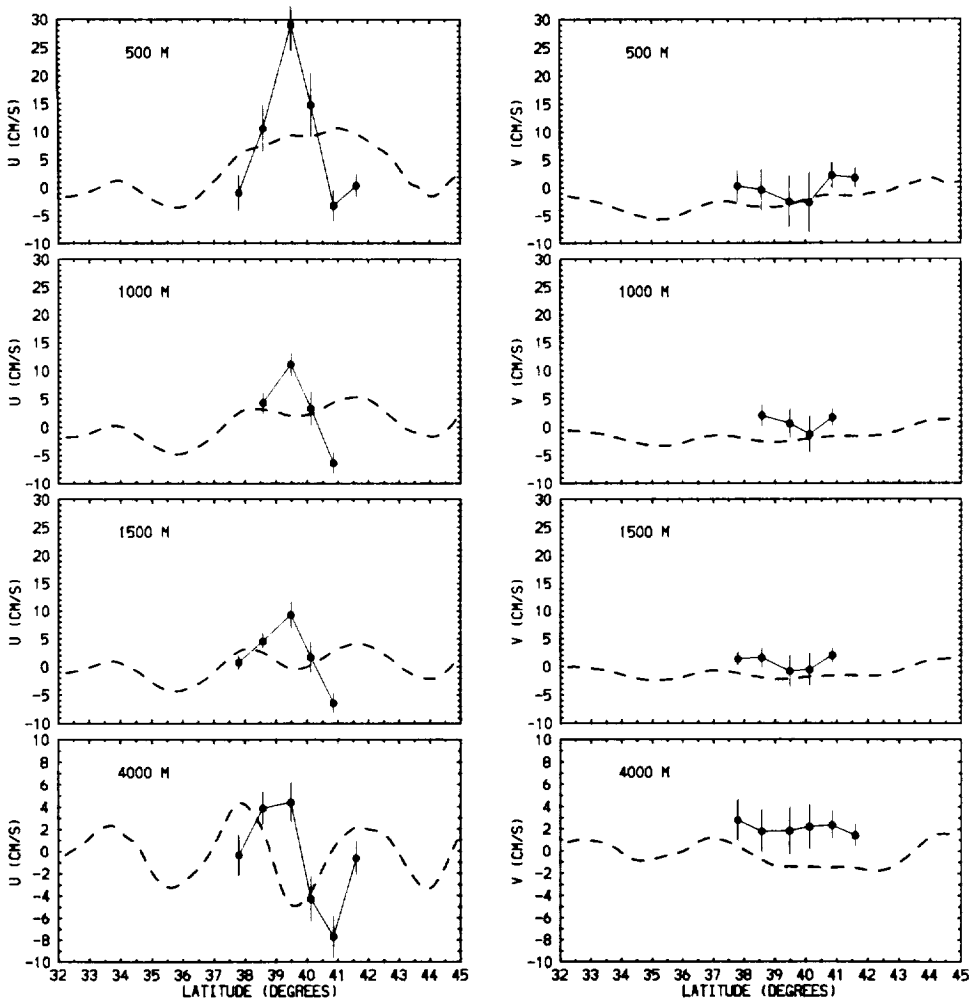

FIG. 15. Comparison between the meridional profiles of velocity components around 55°W from the assimilation results (dashed line) and estimates computed from the current meter measurements at the SYNOP East Array (dots connected by the thin solid line). The left panels show the zonal velocities; the right panels show the meridional velocities. Vertical bars indicate the standard error of the mean.

tropic" character of the eddy-driven flow is limited close to the surface by the surface data constraint that is applied there.

In Fig. 15 we can notice a shift of approximately 1.5° in the two velocity profiles at 4000 m. The velocity structure from the model at this depth is in relatively good agreement in Fig. 13 with the POLYMODE Array II current meter measurements. Hogg (1990) shows that the mean velocity pattern obtained from the SYNOP east array is qualitatively consistent with the pattern from the POLYMODE Array II data. However, the velocity section at 55°W that Hogg has constructed by using both datasets simultaneously shows that a northward shift of the POLYMODE data would yield a more consistent composite section. The reason for these differences in the position of the deep currents is not clear. A displacement of the mean deep Gulf Stream at the times of the two mooring deployments seems to be the most plausible explanation. However, in this case we would expect a better agreement between the deep flow in the assimilation experiment and the measurements at the SYNOP East Array than with the POLYMODE measurements. The time period of the Geosat data that have been assimilated is, in fact, partially overlapping with the time period of the measurements at the SYNOP east array. The Geosat data cover the period November 1986–May 1988, while the SYNOP data are available approximately from September 1987 to August 1989 so that about 260 days of overlapping exist. Richardson (1985) discusses the variability in the position of the deep Gulf Stream over the whole period of the POLYMODE Array II campaign as revealed by its three 9-month deployments. The deep eastward flow shifted approximately 200 km southward over an 18-month period. A similar process might have occurred over the almost 3-year period

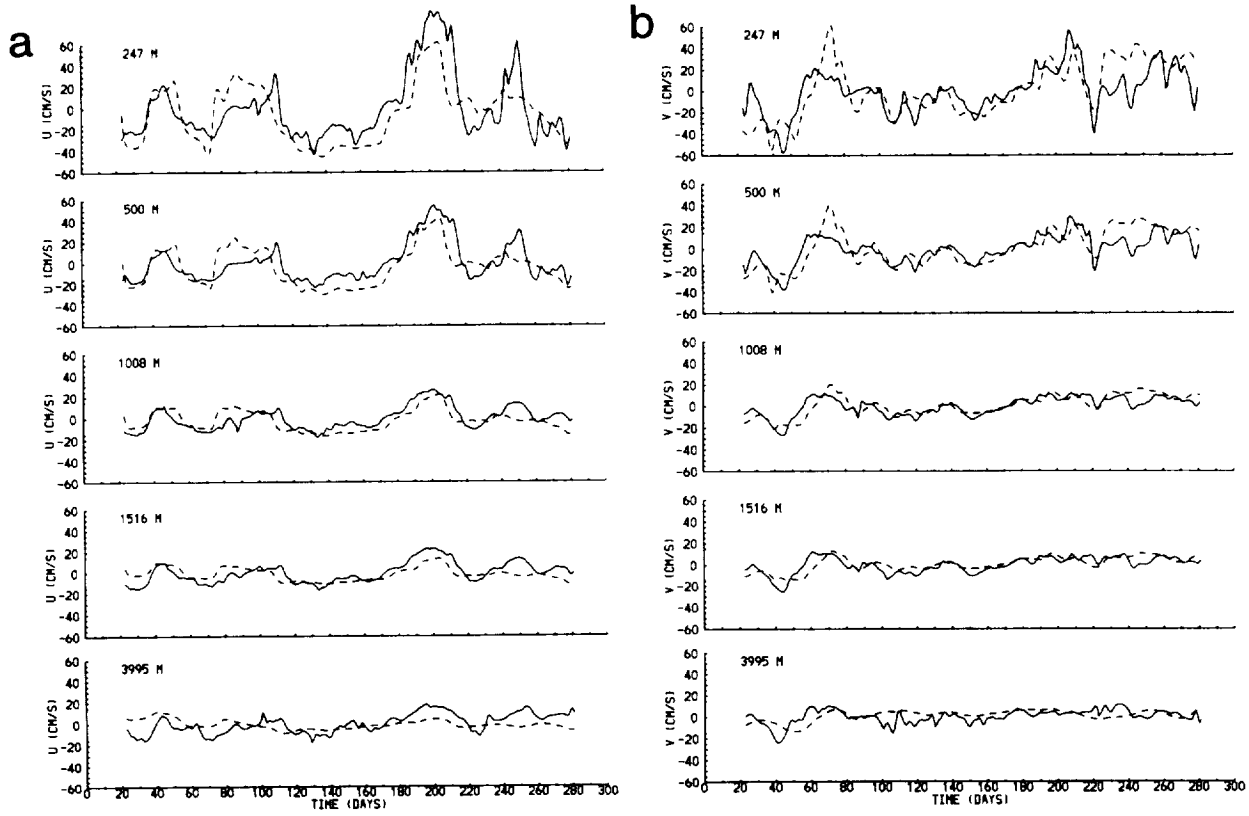

FIG. 16. (a) Comparison between zonal velocity time series measured at 54.67°W, 40.86°N (solid line) and geostrophic zonal velocity time series derived from the assimilation results (dashed line) as a function of depth. The time-averaged velocity has been subtracted from all time series. Day 0 in abscissa corresponds to 1 September 1987. The current meter measurements started on 23 September 1987. The model results have been interpolated linearly to the current meter depths. (b) As in (a) but for the meridional eddy velocity component.

covered by the combination of the Geosat and SYNOP datasets, thus providing a plausible explanation for the shift in the deep flow between the assimilation results and the SYNOP measurements.

These comparisons of mean circulation show the crucial role played by the mean field that is assimilated in determining the structure of the circulation in the subsurface layers. The position of the model Gulf Stream and its southern recirculation are in much better agreement with the observations when incorporating data assimilation. However, the limitations associated with our choice of a climatological field as the missing mean component of the Geosat data, lead to deficiencies in the position, width, and intensity of the subsurface fields in the upper 1500 m. The eddy-driven components of the mean flow, such as the deep Gulf Stream and the southern recirculation, have an amplitude that appears to be in better agreement with the observations. Estimates of the total transport carried by the southern recirculation (Capotondi 1993) seem to be in good agreement with similar estimates computed by Richardson (1985).

b. *The eddy field*

We consider now aspects of the eddy field in the model subsurface layers when the Geosat data are assimilated at the surface. We start this analysis with a direct comparison of the eddy velocity time series measured at the SYNOP East Array with model-derived eddy velocity time series during the overlapping period. We will concentrate, in particular, on the measurements collected at the mooring near 40.86°N, 54.7°W. This mooring is equipped with current meters at five different depths: approximately 250, 500, 1000, 1500, and 4000 m (Table 1). The comparison is shown in Fig. 16.Figure 16a describes the time evolution of the zonal velocities, while Fig. 16b describes the meridional velocity. The solid line indicates the current meter measurements, while the dashed line describes the model geostrophic velocities at the current meter depths. The latter have been computed by linear interpolation between the values at the five model layers. Day 0 on the abscissa corresponds to 1 September 1987. The current meter measurements at this mooring started on 23 September 1987.

The comparison at 247 m shows characteristics similar to the ones observed in the comparison between the current meter measurements and the Geosat data shown in Fig. 3. The most energetic, low-frequency events present in the current meter time series are captured also by the model time series even if discrepancies in amplitude or in phase can sometimes be observed. The quality of the comparison near the surface is thus determined by the characteristics of the Geosat data. The degree of agreement between in situ data and model estimates appears to remain approximately the same at 500, 1000, and 1500 m. The corresponding correlation coefficient is about 0.7. At these depths the velocity signals are approximately equivalent barotropic both in the model and in the data; that is, their amplitudes decrease with depth, but their phase lines are almost vertical. Notice, in particular, the very energetic event that is observed in the zonal velocity record between day 170 and day 220 (corresponding to 16 February and 6 April 1988, respectively). This event seems to be associated with the evolution of an energetic eddy as seen in Fig. 17. In this figure we show the evolution of the geostrophic velocities derived from the Geosat maps from 11 March to 19 March 1988 in a 10° × 10° square containing the location of the current meter mooring (indicated by a dot). Although the zonal velocity appears generally underestimated in the model results, the event can clearly be identified in the model down to 1500-m depth. However, in the deep ocean the comparison seems to degrade. The equivalent barotropic character appears to persist in the data also at 4000 m, while the model signal is almost flat at this depth. The correlation coefficient at this depth is as low as 0.06 for the zonal velocity and 0.2 for the meridional velocity. These considerations are confirmed by the variation of coherences and phases with depth (Capotondi 1993). In section 2 we have noticed that the Geosat time series are coherent with the current meter time series for periods longer than approximately 30 days. The assimilation results show that the coherence between model time series and current meter time series in the same frequency band remains above the significance level at 500, 1008, and 1516 m. At 4000 m, however, the coherence drops below the significance level almost everywhere. How can we explain this result? The possible sources of error in the time-dependent component of the assimilation results can be attributed to three causes: the surface data, the model physics (including vertical stratification), and the resulting model mean potential vorticity fields. In the following we analyze each of these aspects in detail.

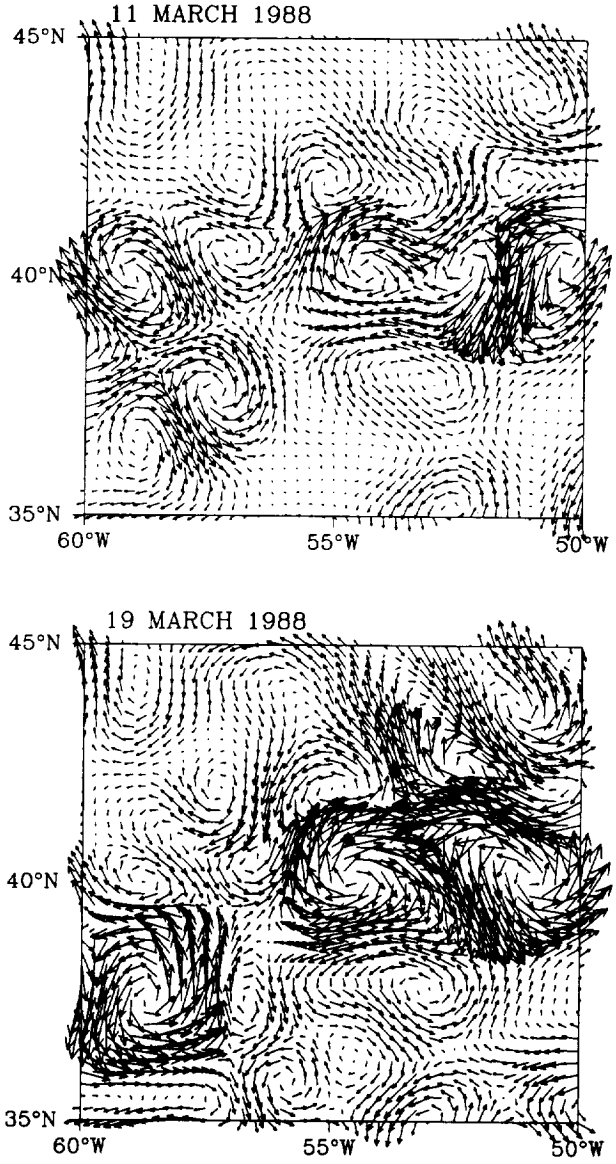

FIG. 17. Instantaneous geostrophic velocity fields derived from the interpolated Geosat data on 11 March 1988 (top) and 19 March 1988 (bottom). The dot at 54.67°W, 40.86°N in each plot indicates the location of the current meter mooring where the time series in Fig. 16 were measured.

1) THE SURFACE DATA

We have seen that the time dependence of the eddy field in the Geosat maps is coherent with in situ measurements over a broad frequency range. An additional aspect that needs to be considered is the frequency–wavenumber relationship. In fact, the spectral components that show a correct time dependence might be associated with incorrect wavenumbers due to aliasing problems. The aliasing issue in the Geosat dataset has been discussed in detail by Wunsch (1989b). A definitive answer is not yet available due to the complex pattern of the satellite measurements. However, we can anticipate, for example, that plane waves with crests parallel to the satellite arcs will be easily aliased to waves with zero wavenumber if the cross-track sampling is too coarse. It can also be shown that waves whose

wavenumber is correctly resolved by the spatial sampling but whose frequency is not resolved by the temporal sampling will be aliased to waves with the same frequency but with a wavenumber of opposite sign. A plane Rossby wave will thus appear as an eastward propagating signal, so that its vertical structure will be surface-trapped even if the real signal were oscillatory with depth. An incorrect frequency–wavenumber relationship can thus be expected to introduce inaccuracies in the vertical structure associated with the surface signal.

2) THE MODEL

The model is based upon the quasigeostrophic approximation. Therefore, it cannot properly represent time-dependent motions associated with ageostrophic processes. The verification of the geostrophic approximation in the Gulf Stream performed by Johns et al. (1989) shows that the largest deviations from geostrophy are associated with high-frequency meandering processes and are found close to the surface. Therefore, ageostrophic phenomena do not seem to be responsible for the discrepancies observed at depth. Another aspect that might affect the model response at depth is the lack of topographic relief. In the area around 40°–41°N, 55°W, no significant bathymetric variation is present, so that this factor may or may not be a crucial one. Can topography at some distance from this site play a role? Probably. A final aspect is the model stratification, namely the vertical resolution and the discretization of the vertical density profile. Several experimental studies (see, for example, Davis 1975; Richman et al. 1977; Owens 1985) have shown that the vertical structure of the mesoscale variability can be described in terms of a few vertical modes so that the model vertical resolution also does not seem to be a major issue. However, an "incorrect" discretization of the basic-state vertical density profile can lead to an incorrect vertical structure of the signal.

3) THE MEAN POTENTIAL VORTICITY FIELDS

The basic-state potential vorticity distributions in the model subsurface layers affect the vertical profile of the time-dependent motion. If, for example, the potential vorticity fields are dominated by the planetary term ($f_0 + \beta y$), the assimilated eddies will be seen by the model as the surface signature of Rossby waves. The resulting vertical structure will be either oscillatory or exponentially decaying, depending on the frequency–wavenumber relationship of the surface signal (Pedlosky 1979). If, on the other hand, the basic-state potential vorticity in the subsurface layers has very weak horizontal gradients, the vertical profile of a surface disturbance can be expected to be equivalent barotropic with almost vertical phase lines. The eddy amplitude decreases exponentially with depth, with an e-folding scale given by the ratio between the first Rossby deformation radius and the horizontal eddy length scale. The current meter time series in Fig. 16 show a decreasing amplitude with depth but no significant phase shift in time. The phase lines are almost vertical. This evidence of an equivalent barotropic character in the observations is consistent with having weak gradients in the mean potential vorticity fields. The current meter measurements in Fig. 16 were recorded at a location in the Gulf Stream where the eddy field is most intense. Therefore, the possibility of a "well mixed" potential vorticity distribution appears plausible, at least on the basis of the potential vorticity dynamics observed in quasigeostrophic models. This hypothesis also seems to be confirmed by the analysis of the SYNOP data performed by Hogg (1992). In our assimilation results the potential vorticity fields in layers 2 and 3 show areas in which the potential vorticity gradients have been eroded by the turbulent eddy field, especially in the Gulf Stream and southern recirculation (Fig. 13 in Part I). In layers 4 and 5, on the other hand, the mean potential vorticity contours are dominated by the βy term in a large part of the domain. At these depths the eddy field appears to be too weak to efficiently mix the potential vorticity. A possible interpretation of the time series comparison in Fig. 16 is that the assimilated eddy field is energetic enough in the upper model layers to effectively alter the mean potential vorticity distributions in some areas. The corresponding vertical profile of the instantaneous surface signals will be equivalent barotropic, in agreement with the current meter measurements. In the two deeper layers, on the contrary, where the potential vorticity fields remain dominated by the planetary vorticity gradients, the eddy signals will disperse as Rossby waves, thus explaining the loss of coherence with the deep current meter data. In other words, eddies will effectively penetrate only to a depth at which their associated currents are strong enough to mix the potential vorticity.

No definite explanation is possible at this point. The scenario we are trying to understand is, in fact, a complex one: there are differences between climatology and eddy fields, and the boundary conditions are steady and closed in the two deeper layers, thus favoring the development of basin-mode-type disturbances as seen in section 3. Furthermore, eddy motion generated by model instabilities and uncorrelated with the surface data may be present in the deeper layers where the surface restoring is not effective. The extent to which these mechanisms are acting during the assimilation experiments and can explain the results obtained needs to be investigated in future studies.

We conclude this section with an analysis of the eddy kinetic energy distributions that are obtained in this assimilation experiment. They are shown in Fig. 18. Only layers 1 (top), 3 (middle), and 5 (bottom) are shown for brevity. The eddy kinetic energy distribution

in the first layer is very similar to the one derived from the interpolated Geosat data, as shown in Fig. 5a. Maximum values are achieved along the mean Gulf Stream path. The eddy kinetic energy decreases away from the stream to values of approximately 100 $cm^2 s^{-2}$, which are found both in the gyre interior and in the area of the continental shelf north of the stream. The maximum values in Fig. 18 tend to be lower than the ones in Fig. 5a. The absolute maximum is observed around 65°W in both cases, but in Fig. 18 it is only 1500 $cm^2 s^{-2}$ instead of 2000 $cm^2 s^{-2}$, as observed in Fig. 5a. This effect is very likely caused by some degree of damping associated with the nudging term or with the other frictional terms present in the model.

In layer 3 (nominal depth 1125 m) maximum values are about 100 $cm^2 s^{-2}$. Also in this case they occur following the mean Gulf Stream path. At this depth, however, the energy level appears to decay more slowly on either side of the maximum. In layer 5 only isolated maxima of about 100 $cm^2 s^{-2}$ can be observed within a large pool of almost uniform eddy kinetic energy with values around 50 $cm^2 s^{-2}$. The eddy kinetic energy appears to decay very slowly toward the border of the domain.

How do these results compare with observations? Several authors (Richardson 1983a; Schmitz 1984; Weatherly 1984) have observed and discussed the kinematical and dynamical links between the eddy kinetic energy distribution and the characteristics of the mean circulation. The observed eddy kinetic energy pattern shows a maximum near the Gulf Stream at all vertical levels. According to Schmitz (1984) the eddy kinetic energy decreases more abruptly into the gyre interior with increasing depth. In the map of surface eddy kinetic energy constructed by Richardson (1983b) and reproduced in Fig. 5b, the ratio between the Gulf Stream and the interior values is about 10. In the deep ocean, on the other hand, the eddy kinetic energy falls off from the Gulf Stream to the interior by two orders of magnitude, ranging from values around 100 $cm^2 s^{-2}$ in the proximity of the Gulf Stream to values of only 1 $cm^2 s^{-2}$ in the interior (Schmitz 1984). An estimate of abyssal eddy kinetic energy computed by Weatherly (1984) is reproduced in Fig. 19. This map was constructed by using measurements recorded at depths much below the main thermocline, typically around 4000 m. Therefore, the distribution in Fig. 19 should be compared with the assimilation results in the model layer 5 whose middle depth is 3900 m.

The comparison between the eddy kinetic energy distribution in the model upper layer (Fig. 18a) with the surface eddy kinetic energy from the drifter data (Fig. 5b) shows a very similar pattern but reduced maximum values in the assimilation results. The lower energy level observed in Fig. 18 can be partially attributed to the characteristics of the assimilated eddy maps. As discussed in section 2, the interpolation procedure used to construct the eddy maps smooths the sea surface height gradients and thus determines a reduction of the geostrophic eddy velocities. Some degree of damping associated with the nudging procedure might be responsible for a further reduction of the upper-layer eddy kinetic energy in the assimilation results.

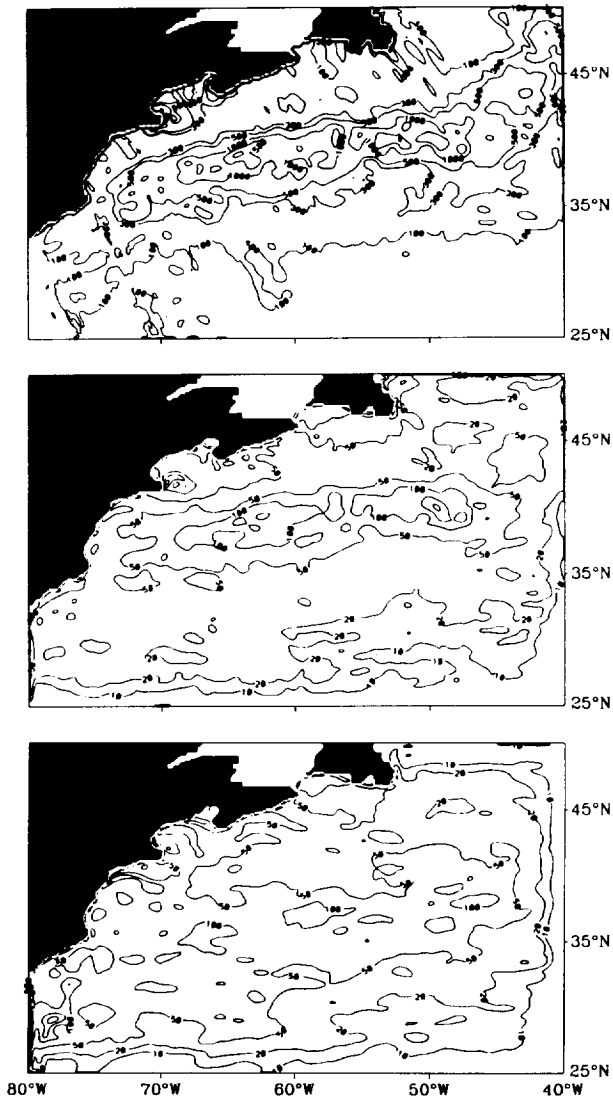

FIG. 18. Eddy kinetic energy distribution in model layers 1 (top), 3 (middle), and 5 (bottom) resulting from the assimilation experiment.

The eddy kinetic energy observed in the fifth model layer (Fig. 18c) has maximum values generally lower than in Fig. 19. Values of 100 $cm^2 s^{-2}$ are found in the model as isolated patches in contrast with the more extensive tongue of values above 100 $cm^2 s^{-2}$ that is observed in Weatherly's map (Fig. 19). Moreover, the general eddy kinetic energy pattern in the model's deepest layer does not show the abrupt decay from Gulf Stream values to interior values that appears in Weatherly's estimate. In the model the abyssal eddy

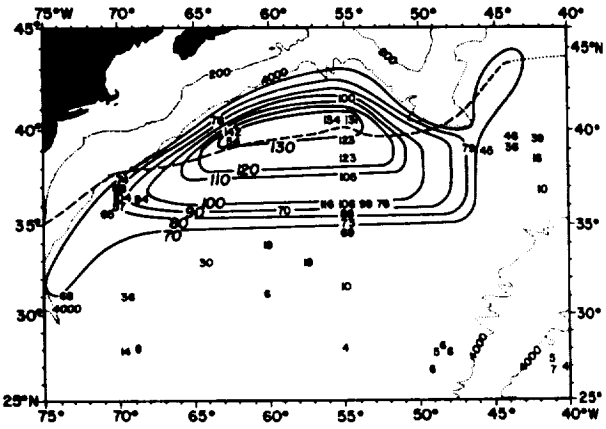

FIG. 19. Distribution of abyssal eddy kinetic energy computed by Weatherly (1984) from current meter measurements much below the main thermocline, typically at 4000-m depth. The dashed line is the landward edge of the surface Gulf Stream as determined by Auer (1982).

kinetic energy tends to remain much more constant than in the data. The possibility that some fraction of eddy energy may excite the barotropic basin modes discussed in section 3 appears as the most likely explanation for the eddy kinetic energy distribution in the model's deepest layers.

5. Discussion and conclusions

We have tried to assess how much closer to reality the model behavior becomes when surface data are assimilated. To this end we have considered aspects of the mean circulation, as well as characteristics of the eddy field. Since the mean component of the surface data is a long-term climatological mean, the representation of the mean circulation that we have adopted is the one derived from an Eulerian time average. The comparison between meridional profiles of mean zonal velocities computed from observations and similar profiles derived from the assimilation results shows a relatively good agreement in the position of both the Gulf Stream and the southern recirculation. The amplitude of the zonal velocity in the Gulf Stream is often underestimated, especially in the upper ocean, where the surface data constraint is most effective. The westward flow associated with the southern recirculation, on the other hand, has amplitudes remarkably similar to the observed ones at almost all depths. This westward flow was not present in the climatological fields used as initial conditions in layers 2 and 3. It appears to be an eddy-driven feature.

The analysis of the eddy field in the assimilation results indicates the potential for the assimilation procedure to produce a realistic time-dependent motion in the model subsurface layers. Comparison with in situ data measured during the same period of time shows, in fact, a relatively good agreement. A coherence above the significance level is obtained down to about 1500-m depth in a frequency band that is established by the spectral characteristics of the surface data. The eddy kinetic energy appears to be underestimated in the model results. This can partially be explained with the reduced energy level in the interpolated Geosat data that are assimilated, especially at high wavenumbers.

The main conclusion that can be drawn from the comparisons we have described is that nudging of a model with altimeter data appears to be a very promising tool for driving ocean models toward a more realistic behavior. This includes climatological aspects, as well as aspects related to the temporal evolution of the model fields. We have seen that the imposition of a surface data constraint can radically alter the model behavior at all depths. The deficiencies that we have detected in the assimilation results can be largely attributed to limitations present in the data that have been used, in particular the mean climatological component. Most of the characteristics of the mean model circulation that appear in disagreement with the observations (width and intensity of the eastward-flowing jet, limited development of the northern recirculation gyre, etc.) can, in fact, be attributed to inadequacies in the mean climatological component. Further improvements in the assimilation results thus require a more adequate surface mean field. Future work must include the analysis of the performance of different mean fields, as well as the investigation of techniques that allow the assimilation of only the eddy component of the data. In the present analysis we have also identified a model limitation, which is the inadequate treatment of the open boundary conditions; this limitation can be improved by implementing radiation boundary conditions at all the open boundaries. Some of the deficiencies in the present results may also be due to inadequacies in the quasigeostrophic approximation. In particular, the possibility of including a finite topography, as well as the inclusion of thermodynamic forcing (Ezer and Mellor 1992), may improve the model performance considerably. Future studies of this type, therefore, should be extended to primitive equation models.

Acknowledgments. We would like to thank Drs. Victor Zlotnicki and Lee Fu for making the Geosat data available to us and Dr. Nelson Hogg for kindly supplying the current meter data at the Synop East Array. Steve Worley, NCAR data support section, helped with the dynamic height computation. Julianna Chow supplied very precious assistance in the computational aspects of this work. One of us (AC) would like to thank Drs. Joe Pedlosky, Carl Wunsch, and Mindy Hall for the stimulating ideas and constructive criticism they have supplied during the course of this work; AC would also like to thank the NCAR Advanced Study Program for giving her the opportunity to carry out large parts of this work at NCAR. This

study was supported by NASA through Contract 958208 with the Jet Propulsion Laboratory, NASA Grant NAGW2711 with MIT (PMR), and subcontract W-16 351B with the Jet Propulsion Laboratory to NCAR (WRH) as a part of the TOPEX-Poseidon investigation.

REFERENCES

Auer, S. J., 1982: Gulf Stream System boundary statistics from the NWS/NESS Dayly Oceanographic Analysis. *Trans. Amer. Geophys. Union*, **63**, 363.

Capotondi, A., 1993: Assimilation of altimeter data in a quasi-geostrophic model of the Gulf Stream system: A dynamical perspective. Ph.D. thesis, MIT-WHOI Joint Program, 238 pp.

——, P. Malanotte-Rizzoli, and W. R. Holland, 1995: Assimilation of altimeter data into a quasigeostrophic model of the Gulf Stream system. Part I: Dynamical construction. *J. Phys. Oceanogr.*, **25**, 1130–1152.

Davis, R. E., 1975: Statistical methods, *Dynamics and the Analysis of MODE-I: Report of the MODE-I Dynamics Group*, Massachusetts Institute of Technology, Cambridge, MA, 1-26 (unpublished document).

Ezer, T., and G. L. Mellor, 1992: A numerical study of the variability and the separation of the Gulf Stream, induced by surface atmospheric forcing and lateral boundary flows. *J. Phys. Oceanogr.*, **22**, 660–682.

——, D. S. Ko, and G. L. Mellor, 1992: Modeling and forecasting the Gulf Stream. *Mar. Technol. Soc. J.*, **26**(2), 5–14.

——, G. L. Mellor, D. S. Ko, and Z. Sirkes, 1993: A comparison of Gulf Stream sea surface height fields derived from Geosat altimeter data and those derived from sea surface temperature data. *J. Atmos. Oceanic Technol.*, **10**, 76–87.

Ghil, M., and P. Malanotte-Rizzoli, 1991: Data assimilation in meteorology and oceanography. *Advances in Geophysics*, Vol. 33, Academic Press, 141–266.

Hall, M. M., and H. L. Bryden, 1985: Profiling the Gulf Stream with a current meter mooring. *Geophys. Res. Lett.*, **12**, 203–206.

Hogg, N. G., 1990: Some early impressions from SYNOP East. *The SYNOPticians*, **1**(5).

——, 1992: On the transport of the Gulf Stream between Cape Hatteras and the Grand Banks. *Deep-Sea Res.*, **39**, 1231–1246.

Holland, W. R., 1978: The role of mesoscale eddies in the general circulation of the ocean-numerical experiments using a wind-driven quasigeostrophic model. *J. Phys. Oceanogr.*, **8**, 363–392.

——, and W. J. Schmitz Jr., 1985: Zonal penetration scale of model midlatitude jets. *J. Phys. Oceanogr.*, **15**, 1859–1875.

Johns, E., D. R. Watts, and H. T. Rossby, 1989: A test of geostrophy in the Gulf Stream. *J. Geophys. Res.*, **94**(C3), 3211–3222.

Le Traon, P. Y., M. C. Rouquet, and C. Boissier, 1990: Spatial scales of mesoscale variability in the North Atlantic as deduced from Geosat data. *J. Geophys. Res.*, **95**(C11), 20 267–20 285.

Lozier, M. S., and S. C. Riser, 1990: Potential vorticity sources and sinks in a quasigeostrophic ocean: Beyond western boundary currents. *J. Phys. Oceanogr.*, **20**, 1608–1627.

Marshall, D., and J. C. Marshall, 1992: Zonal penetration scale of midlatitude oceanic jets. *J. Phys. Oceanogr.*, **22**, 1018–1032.

Marshall, J. C., 1984: Eddy-mean-flow interaction in a barotropic ocean model. *Quart. J. Roy. Meteor. Soc.*, **110**, 573–590.

Mellor, G. L., and T. Ezer, 1991: A Gulf Stream model and an altimetry assimilation scheme. *J. Geophys. Res.*, **96**, 8779–8795.

Owens, B. W., 1985: A statistical description of the vertical and horizontal structure of eddy variability on the edge of the Gulf Stream recirculation. *J. Phys. Oceanogr.*, **15**, 195–205.

——, 1991: A statistical description of the mean circulation and eddy variability in the northwestern Atlantic using SOFAR floats. *Progress in Oceanography*, Vol. 28, Pergamon, 257–303.

——, and N. G. Hogg, 1980: Oceanic observations of stratified Taylor columns near a bump. *Deep-Sea Res.*, **27**, 1029–1045.

Pedlosky, J., 1979: *Geophysical Fluid Dynamics*. Springer-Verlag, 624 pp.

Rhines, P. B., and R. Schopp, 1991: The wind-driven circulation: Quasigeostrophic simulations and theory for nonsymmetric winds. *J. Phys. Oceanogr.*, **21**, 1438–1469.

Richardson, P. L., 1983a: A vertical section of eddy kinetic energy through the Gulf Stream system. *J. Geophys. Res.*, **88**(C4), 2705–2709.

——, 1983b: Eddy kinetic energy in the North Atlantic from surface drifters. *J. Geophys. Res.*, **88**(C7), 4355–4367.

——, 1985: Average velocity and transport of the Gulf Stream near 55°W. *J. Mar. Res.*, **43**, 83–111.

Richman, J. G., C. Wunsch, and N. G. Hogg, 1977: Space and time scales of mesoscale motion in the western North Atlantic. *Rev. Geophys. Space Phys.* **15**, 385–420.

Schmitz, W. J., Jr., 1984: Abyssal eddy kinetic energy in the North Atlantic. *J. Mar. Res.*, **42**, 509–536.

——, and W. R. Holland, 1982: A preliminary comparison of selected numerical eddy-resolving general circulation experiments with observations. *J. Mar. Res.*, **40**, 75–117.

——, and M. S. McCartney, 1982: An example of long term variability for subsurface currents and hydrographic patterns in the western North Atlantic. *J. Mar. Res.*, **40**(Suppl.), 707–726.

——, and W. R. Holland, 1986: Observed and modeled mesoscale variability near the Gulf Stream and Kuroshio extension. *J. Geophys. Res.*, **91**(C8), 9624–9638.

——, and J. D. Thompson, 1993: On the effects of horizontal resolution in a limited area model of the Gulf Stream System. *J. Phys. Oceanogr.*, **23**, 1001–1007.

Thompson, J. D., and W. J. Schmitz Jr., 1989: A limited-area model of the Gulf Stream: Design, initial experiments, and model-data intercomparison. *J. Phys. Oceanogr.*, **19**, 791–814.

Weatherly, G. L., 1984: An estimate of bottom friction dissipation by Gulf Stream fluctuations. *J. Mar. Res.*, **42**, 289–301.

Wunsch, C., 1989a: Tracer inverse problems. *Oceanic Circulation Models: Combining Data and Dynamics*, D. L. T. Anderson and J. Willebrand, Eds., Kluwer, 1–77.

——, 1989b: Sampling characteristics of satellite orbits. *J. Atmos. Oceanic Technol.*, **6**, 891–907.